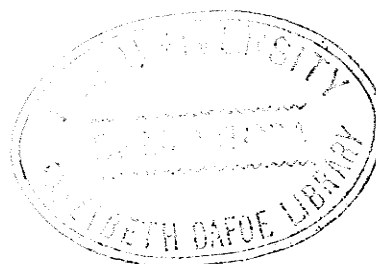


RADIATION DOSIMETRY
EMPLOYING THE
THERMOLUMINESCENCE OF LITHIUM FLUORIDE

A Thesis
Submitted to
the Faculty of Graduate Studies
University of Manitoba

In Partial Fulfillment
of the Requirements for the Degree
Master of Science

by
Ronald G. Worton
October, 1965.



RADIATION DOSIMETRY
EMPLOYING THE
THERMOLUMINESCENCE OF LITHIUM FLUORIDE

Ronald G. Worton

ABSTRACT

The radiation induced thermoluminescence of LiF has been studied using a commercially available system based on this phenomenon. The response characteristics of the LiF to x-rays generated at 100 kv. and 250 kv., to gamma rays from Co^{60} , and to electrons from 25 Mev. to 35 Mev. have been investigated, and response curves have been presented for future clinical applications. An important, new characteristic, increased energy dependence with higher doses, was discovered, and a simple model has been presented to explain this.

A method of obtaining glow curves using low heating rates has been developed, and by comparison with glow curves obtained with larger heating rates (250 degrees/min.), a trap depth of 3.0 ev. was determined for the main traps in LiF.

The LiF has been studied to determine the extent of the fading of the stored energy at room temperature, to determine the effects of annealing the crystals prior to use and to determine the extent of permanent radiation damage to the LiF.

The literature on thermoluminescence in LiF has been carefully reviewed, and the absorption and measurement of therapeutic radiation has been outlined. The extent of the knowledge of the mechanism of action of thermoluminescence in LiF has also been presented.

ACKNOWLEDGEMENTS

The work to be described in this thesis was carried out as part of the research program at the Manitoba Cancer Treatment and Research Foundation under the direction of Dr. A. F. Holloway. The author is particularly indebted to Dr. Holloway for his invaluable instruction and supervision. Grateful acknowledgement is also extended to the staff at the Foundation for their assistance, and to Dr. I. Cooke for supplying some of the LiF that was studied.

The financial support of the Manitoba Cancer Treatment and Research Foundation, and of the National Cancer Institute of Canada is gratefully acknowledged.

TABLE OF CONTENTS

CHAPTER	PAGE
I. INTRODUCTION	1
II. RADIATION - ABSORPTION AND MEASUREMENT	13
A. Electromagnetic Radiation	13
(1.) Interaction with matter	13
(a.) Classical or Rayleigh scattering	16
(b.) Photoelectric effect	17
(c.) Compton process	18
(d.) Pair production	20
(2.) Detection and measurement	21
(a.) Definition of the roentgen	21
(b.) Absorbed dose	22
(c.) Measurement of exposure in roentgens	23
B. Electrons	26
(1.) Interaction with matter	26
(2.) Detection and measurement	27
III. THERMOLUMINESCENCE IN LITHIUM FLUORIDE	28
A. Energy bands, traps, and glow curves	28
(1.) Band theory applied to LiF	28
(2.) Trapping levels	28
(3.) Glow curves or thermoluminescence curves	29

CHAPTER	PAGE
B. Trapping centers in lithium fluoride	31
IV. APPARATUS AND PRELIMINARY OBSERVATIONS	34
A. Apparatus	34
B. Preliminary observations	37
(1.) Digital voltmeter	37
(2.) Phosphor dispenser	38
(3.) Response to 100 roentgens	38
(4.) Powder distribution in the planchet	39
(5.) Power requirements to planchet	40
V. EXPERIMENTAL METHODS AND RESULTS	42
A. Calibration curves	42
(1.) Cobalt calibration	43
(2.) X-ray calibration	48
(3.) Electron calibration	50
B. Statistical analysis	56
C. Annealing procedure	61
D. Glow curves	63
E. Trap depth	66
F. Fading of stored energy	71
G. Response of other LiF	76
VI. CONCLUSIONS	78
BIBLIOGRAPHY	83
APPENDIX A. CALCULATION OF ABSORPTION COEFFICIENTS	86
APPENDIX B. CALCULATION OF STOPPING POWERS	87

LIST OF FIGURES

FIGURE	PAGE
1. Mechanism of Thermoluminescent Dosimeters	6
2. Apparatus	35
3. Co^{60} Calibration	45
4. Co^{60} Calibration	46
5. X-Ray Calibration	49
6. X-Ray Response Relative to Co^{60}	51
7. Electron Calibration	52
8. Electron - Co^{60} Comparison	55
9-A. Sample Averages at 100 Rads	59
9-B. Sample Averages at 1000 Rads	59
10. Energy Remaining vs. Temperature	65
11. Glow Curves	67
12. $\ln I$ vs. $1/T$	69
13. Fading of Type-N LiF	72
14. Fading of Type-7 LiF	75
B-1. Density Correction	92
B-2. Mass Stopping Powers	93

CHAPTER I

INTRODUCTION

The subject of radiation dosimetry has its origins in the last years of the nineteenth century when x-rays, then newly discovered, were almost immediately put to medical use. Both the successes, like that of the first recorded tumor treatment in 1899, and the failures of those early attempts underlined the necessity for some quantitative measurement of the radiation emanating from an x-ray tube.

Most of the early workers used photographic or fluorescence methods for measuring x-ray intensities. Chemical and calorimetric methods were also tried. For reasons of lack of sensitivity, of unreliability, or of unwanted energy dependence, these early physical techniques were eventually displaced by ionization methods. Three decades then passed before an internationally acceptable method of defining and measuring an x-ray dose was achieved. The introduction of the roentgen in 1928 standardized measurements of x-ray intensities around the globe.

In recent years problems of radiation dosimetry

have multiplied rapidly with the vast production of artificial radioactive materials by reactors and the increasing use of high voltage accelerators of various kinds. The energy ranges have been expanded considerably and electron, proton, and neutron beams find an increasing variety of important applications. The measurement of radiation has gone beyond the scope of the roentgen, and now, more than ever, it is necessary to determine the physical energy deposition in a variety of media when irradiated by any one of a wide energy range of quanta, or by any type of ionizing particle. Modern versions of some of the earlier methods, notably chemical and calorimetric methods, are gaining an important place in radiation dosimetry.¹

Solid state devices are becoming increasingly popular in the field of radiation dosimetry. There are many such devices operating on a variety of principles, but none of them gives an absolute measurement of absorbed energy. They must be calibrated under appropriate conditions against a calorimeter, a standard air chamber, or some other absolute device.

Solid state dosimeters are useful for four main reasons:^{2,3} (1.) their high density (800 to 4000 times more atoms per cm^3 than air) leads to small sizes;

(2.) changes induced in solids by radiation may persist for long periods enabling total dose to be estimated at a convenient time after the irradiation; (3.) solid systems that show an obvious visible change are useful for measuring spatial dose distributions; and (4.) higher dose rates can be measured with solid state dosimeters than with ionization chambers.

Many solid state dosimeters work in the following way. ^{2,3,4} Electrons or holes freed by ionization of atoms in solids * can cause induced electrical conductivity while they move through the solid. These carriers eventually recombine or become trapped at localized sites such as impurity atoms or crystal defects. If light is given off in the recombination, the solid is a scintillator. The number of scintillations provides a measure of absorbed energy. If the depth of the traps - the energy needed to release an electron or hole from them - is greater than about 1 eV , the carriers remain in the trapping site for a long time (at least several hours). This site may then absorb light at different wavelengths from the unirradiated solid, or it may alter the luminescent response of the solid to ultra-violet light (radiophotoluminescence). One can also

* Mechanism to be described in more detail in a later chapter.

detect the presence of unpaired electrons by electron-spin resonance. In some solids the stably trapped electrons can be released at a convenient readout time by heating the solid. If the release gives rise to a burst of emitted light, the phenomenon is called thermoluminescence. A more detailed description of each of these mechanisms follows.

For dosimetry using optical absorption the measured quantity is the change in optical density at a suitable wavelength using a spectrophotometer or densitometer. The change in optical density is proportional to the number of new centers created by the ionizing radiation. The useful materials for such a dosimeter are activated glasses, clear plastics, and dyes.

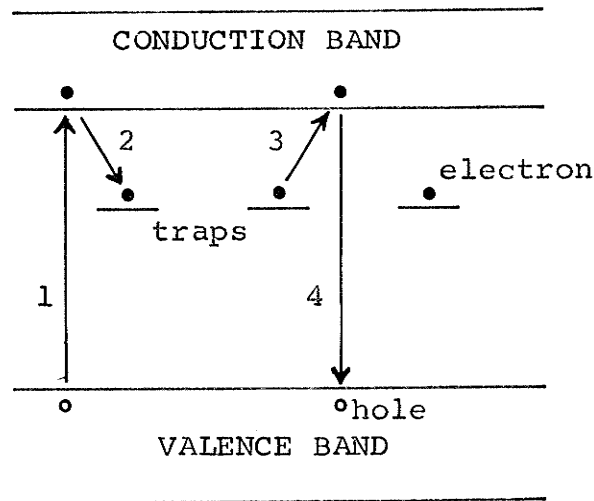
In radiophotoluminescence the trapping center absorbs ultra-violet and emits visible light continuously while the U.V. is on. The intensity of this light is measured and gives a measure of the absorbed dose in the solid, usually a glass.

The number of unpaired electrons produced in powdered alanine by ionizing radiation is measured with an electron spin resonance spectrometer and compared to a standard specimen to obtain an estimate of absorbed dose in the alanine. This system has been used in artificial satellites with an accuracy of about 5%.

Semiconductor junction detectors behave much like solid state ionization chambers. Ionizing radiation generates pairs of charge carriers in the depletion region which are collected by a potential across this region. Conductivity can also be induced in CdS, plastics, and organic insulators by ionizing radiation.

Thermoluminescence provides a system more sensitive than any of the above. When a thermoluminescent material such as $\text{CaF}_2:\text{Mn}$, $\text{CaSO}_4:\text{Mn}$, or LiF , is exposed to ionizing radiation some of the freed electrons are trapped at lattice imperfections in the crystalline solid. They remain trapped for long periods at room temperature. If the temperature is raised the electrons are thermally released from the traps and recombine with oppositely charged centers, with the emission of light. The total quantity of light emitted as the material is heated up can be measured and related to the absorbed dose in the material. (Fig. 1.). CaSO_4 has been used in this way but fading of the effect was severe due to the rapid escape of some electrons from traps at room temperature. Natural $\text{CaF}_2:\text{Mn}$ was better but still required post-irradiation heat treatment to empty the "shallow" traps. Synthetic $\text{CaF}_2:\text{Mn}$ has been made without the shallow traps but a spurious thermoluminescence equivalent to about one roentgen prevented measurements in

FIGURE 1.



MECHANISM OF THERMOLUMINESCENT DOSIMETERS

STEPS.

- (1.) Ionization raises electron from valence band to conduction band.
- (2.) Electron may fall into localized trap.
- (3.) Electron is thermally excited out of trap.
- (4.) Electron de-excites to ground emitting light.

the milliroentgen range. The fading in LiF is much less than in either of these crystals.

In a review of solid state dosimetry (1963), J. F. Fowler² states: "At the moment there is no really satisfactory and generally available small integrating dosimeter for clinical measurements or radiobiological experiments in the range 1 - 10,000 rads *.....Thermoluminescence in lithium fluoride appears to be the most promising system for clinical or radiobiological use, with its quantum energy independence and its range of about 0.1 to 10⁵; it is now commercially available."

An active group of physicists, chemists, and radiologists at the University of Wisconsin has done much to further the cause of LiF as a dosimeter. Prior to 1957 Daniels et al studied LiF extensively^{5,6,7} to determine its response to gamma rays, electrons, alpha particles, and neutrons, and to try to elucidate the nature of the trapping centers in LiF. Then in 1961 Cameron, Daniels, Johnson, and Kenney⁸ announced the construction of a readout instrument for integrating the light given off by the LiF. They used powdered LiF, prepared by grinding and mixing pure fused LiF in order to average out chemical and physical inhomogeneities. A measured volume of powder was irradiated and then placed under a photomultiplier tube. It was heated to 250°C in less than

* One rad is an absorbed dose of 100 ergs per gram

one minute. The light intensity was integrated by collecting the photomultiplier current on a capacitor, and then measuring the voltage on the capacitor with an electrometer voltmeter. (This is precisely the technique adopted by Controls For Radiation Inc., the manufacturer of the instrument now in use at the Manitoba Cancer Foundation - the instrument to be described in this paper.) Cameron and his colleagues made no attempt to control the concentration of luminescent activators in their LiF. They found that these inert, insoluble, and nontoxic crystals of LiF are relatively free from mechanically induced luminescence; they have an almost linear response to amounts of radiation from a few milliroentgens to many kiloroentgens; and because of the low atomic number of both lithium and fluorine, the energy dependence is small compared with that of other dosimeters. They found that over the range from x-rays of 40 kev. effective energy to the 1.1 and 1.3 Mev gamma rays from Co^{60} , the thermoluminescent response varies by only 40%. (Other common dosimeters such as $\text{CaF}_2:\text{Mn}$, film badges, and silver activated phosphate glass, increase in response by about 500% in going from Co^{60} energies to 100 kev. x-rays.) They also found a less than measurable fading at 50°C for 1 day, and reproducibility of readings with a standard deviation of 2%. They used the LiF successfully to measure absorbed dose in the rectum of a patient receiving

internal radiation treatment.

Since 1961 an activated LiF material has been developed especially for thermoluminescent radiation dosimetry (TLD-100 and TLD-700 from the Harshaw Chemical Company, Cleveland, Ohio.) Cameron and his colleagues, using this powder, have developed a technique for determining effective energy of x-ray beams by comparing its response with that of Al_2O_3 which has a different energy response⁹, and have devised an annealing procedure which enables the LiF powder to be reused many times.^{10,11,12}

Many other researchers, using somewhat different readout instruments and different techniques have investigated the thermoluminescence of LiF^{13,14,15} and have confirmed most of Cameron's work. They have found a nearly linear relationship between response and dose¹⁴, wide dose rate independence up to 2.5×10^5 rads/ sec^{13,14}, permanent damage to the LiF after accumulated doses of about 3×10^4 rads^{14,15}, the annealing procedure of Cameron before reuse of the powder to be both necessary and sufficient, standard deviations of four to six measurements to be 1 to 6%, and a limited response to fast neutrons. Cameron himself reports that thermal neutrons give about 50 times greater response (per rad "in tissue") than gamma or x-rays¹⁰. (This response is due to a $Li^6(n,\alpha)H^3$ reaction and the cross section for thermal neutrons is large. TLD-100 contains natural

abundances of Li isotopes (7.4% Li^6 and 92.6% Li^7) while TLD-700 is enriched to at least 99.91% Li^7 . Hence TLD-700 has a much smaller response to thermal neutrons.)

So far in this introductory chapter an attempt has been made to inform the reader of the reasons for relying upon solid state systems for the measurement of absorbed doses of ionizing radiation and to present to the reader, in a simplified model, the mechanism of action of these systems. Thermoluminescence has been introduced in a little more detail, and the advantages of LiF over the other thermoluminescent materials have been presented. The important properties and response characteristics of LiF have been summarized, and the reader is referred to the literature for further details.

Most of the more recent work has been with TLD-100 and TLD-700. In general, the findings of the various researchers agree with one another. However, there are some differences in response curves, and energy dependence measurements, probably due to differences in technique for measuring the light output of the LiF. There may also be differences in activator concentration from one batch of LiF to another.

The LiF being used in this laboratory was supplied by Con-Rad (Controls for Radiation, Inc.) and is not the same

as TLD-100 and TLD-700. This LiF is purchased as Con-Rad type-N (natural abundances of Li isotopes) and Con-Rad type-7 (enriched in Li⁷ to 99.993%.) Thus, the results of experiments performed with TLD-100 or TLD-700 could not be applied to our LiF. At the time of purchase of the Con-Rad system, very little work had been done with electrons. The precision and accuracy for electrons had not been measured, no measurements had been made below 150 rads or above 5,000 rads with electrons, and all that was known about energy dependence was that it was less than 10% between 6 Mev and 19.5 Mev.¹⁶ The light output for electrons had been found to be within 10% of equivalent gamma on a rad per rad basis.¹⁶

Because of these and other uncertainties, and because our LiF was to be used for electron beam measurements, it was felt that a systematic investigation into the characteristics of our LiF and the associated readout apparatus was a very worthwhile project. The author was asked in the spring of 1964 to undertake such a project, and the work to be described was performed between the spring of 1964 and the fall of 1965.

Because of the nature of this project there are several short and seemingly unrelated experiments that are, however, necessary for a complete understanding of the dosimeter system. These will be reported, as well as a

study of the theoretical considerations involved in accurately comparing response to electrons with response to Co^{60} . A complete calibration of the dosimeter for x-rays, Co^{60} , and electrons will be presented.

Chapter II of this dissertation will introduce some fundamental ideas concerning therapeutic radiation, its production, its interaction with matter, and its detection. Chapter III will present the mechanism of trapping and releasing energy in LiF , at least as much as is known of this mechanism. Chapter IV will describe the apparatus and some of the preliminary experiments. The main experimental results will be presented in Chapter V, and frequent reference will be made to the material presented in Chapters II, and III.

CHAPTER II

RADIATION - ABSORPTION AND MEASUREMENT

The therapeutic radiations with which we shall be concerned are (1.) x-rays (electromagnetic radiation) with energies up to 250 kev, (2.) gamma rays (electromagnetic radiation) from a Co⁶⁰ teletherapy unit, and (3.) electrons of energies from 10 Mev. to 35 Mev. from a betatron. The x-radiation is characterized by the fact that its energy distribution consists of line spectra (characteristic x-rays) superimposed on a diffuse background of bremsstrahlung. The characteristic x-rays are due to electronic transitions to the innermost shells of the atoms of the target material, and the bremsstrahlung radiation is due to the deceleration of high energy electrons by "collisions" with nuclei. There are two monochromatic gamma rays of energies 1.33 Mev. and 1.17 Mev. emitted by Co⁶⁰.

A. ELECTROMAGNETIC RADIATION

(1) Interaction with matter¹⁷

Electromagnetic radiation may react with matter in several ways: it may be deflected or scattered by the

electrons of an atom, it may give up part or all of its energy to an electron, or it may react with the Coulomb field of the nucleus to produce an electron-positron pair. Other interactions, with the nucleus, or with the meson field of the nucleus, are negligible in the energy range with which we are concerned.

Consider a collimated source of radiation, S, an absorber of thickness x , and a collimated detector D. The intensity of radiation, I , as measured by D is found to be given by

$$I = I_0 e^{-ux} \dots\dots\dots (1.)$$

where u is the linear absorption coefficient in cm^{-1} and I , the intensity, is the rate of energy flow across unit area in $\text{ergs/cm}^2 - \text{sec}$.

It is evident that the detector will give a measure of all the radiation that has been removed from the beam, whether this has been truly absorbed, or simply deflected out of its range. Therefore, u , as determined by this measurement, is the total absorption coefficient, and should be distinguished from the true or real absorption coefficient, u_a , which is a measure of the energy actually absorbed in the material.

If thickness in equation (1.) is to be measured in terms of grams / cm^2 , then u must be replaced by u / ρ ,

the mass absorption coefficient, where ρ is the density of the absorber. Since the interaction of radiation with matter involves the electrons and atoms of the material it is often more useful to obtain the absorption coefficient per electron or per atom. These are all related by means of the density, ρ , the atomic number, Z , the atomic weight, A , and Avogadro's number, $N = 6.02 \times 10^{23}$.

Linear absorption coefficient	=	u	cm^{-1}
Mass	"	"	$= u / \rho \quad \text{cm}^2 / \text{gm}$
Atomic	"	"	$= (u/\rho) (A/N) \text{ cm}^2 / \text{atom}$
Electronic	"	"	$= (u/\rho) (A/N) (1/Z) \text{ cm}^2 / \text{electron}$

The electronic absorption coefficient is sometimes written as ${}_e u$, and the atomic coefficient as ${}_a u$, and since they have the dimensions of area, they represent the cross section per electron and per atom for an interaction.

Within the energy range with which we are concerned, four processes of interaction between radiation and matter are recognized: (a) Classical or Rayleigh scattering, (b) photoelectric effect, (c) Compton process, and (d) pair production, although classical scattering is really a special case of the Compton process. The absorption coefficient, u , may be separated into component coefficients.

$$u = \tau + \sigma + K \dots \dots \dots (2.)$$

where τ is the coefficient for photoelectric effect, σ for the Compton process, and K for pair production.

(a) Classical or Rayleigh scattering

When an electromagnetic wave passes over an electron the electron is made to oscillate with the frequency of the wave, and it in turn radiates energy in the form of a scattered electromagnetic wave of the same wavelength as the primary. The phenomenon has been called coherent scattering, since the scattering actions of different atomic electrons can combine coherently. The differential cross section for the process was derived by Thomson and is given by¹⁸

$$\frac{d_e \sigma}{d\Omega} = \frac{e^4}{2m_0^2 c^4} (1 + \cos^2 \phi) \dots \dots \dots (3.)$$

where e is the electronic charge, m_0 the electron mass, and c the velocity of light; $d_e \sigma / d\Omega$ is the differential cross section per unit solid angle and gives the fraction of the incident energy which is scattered by an electron into unit solid angle, $d\Omega$, at angle ϕ . Putting $d\Omega = 2\pi \sin \phi d\phi$ and integrating over all angles from $\phi = 0$ to $\phi = \pi$, one obtains the total electronic cross section (or absorption coefficient) for classical scattering, $e\sigma_0$, which is given by

$$e\sigma_0 = \int_{\phi=0}^{\phi=\pi} d_e \sigma = \frac{8}{3} \frac{e^4}{m_0^2 c^4} = 6.65 \times 10^{-25} \text{ cm}^2 \dots \dots \dots (4.)$$

It contributes to the total, but not to the real absorption

coefficient. (This classical scattering coefficient is an oversimplification of the true state of affairs. It should be modified by an energy dependent scattering factor to take into account interference effects of the coherently scattered photons.¹⁸⁾

(b) Photoelectric effect

When the energy, $h\nu$, of the incident photon is greater than the binding energy, ϕ , of the atomic electrons, a direct collision may result in complete absorption of the photon, and ejection of a photoelectron of energy $h\nu - \phi$. After the electron has been ejected, the atom is left in an excited state due to a vacancy in the K or L shell. An outer electron drops into the vacancy, and a fluorescent light is emitted of energy $h\nu = \phi$. The photoelectron is locally absorbed, but the fluorescent light may not be if ϕ is large enough. The binding energy of the K shell in lead is 88 kev. and a photon of this energy could escape from the material. However, in tissue-like materials where binding energies are less than 500 ev., all the fluorescent photons will be re-absorbed, and hence in these materials the total absorption coefficient τ and the real absorption coefficient τ_a will be identical.

The electronic cross section for this process is a maximum when $h\nu$ is slightly greater than ϕ , but as $h\nu$ increases, τ_e decreases rapidly (approximately as $h\nu^{-3}$).

In the energy region above the absorption edge the cross section per electron varies approximately as Z^3 , and so is most prominent in the heavy materials such as lead.¹⁹

(c) Compton Process

A Compton process takes place with "free" electrons, and hence predominates when the photon energy, $h\nu$, is large compared to the binding energy of the atomic electrons. A photon of energy $h\nu$ sets the electron in motion and is itself scattered with reduced energy $h\nu'$. The electron and photon are considered as a closed system and hence energy and momentum are conserved. The electron goes off at an angle θ to the direction of the incident photon, with a relativistic mass $m = m_0 / \sqrt{1 - \beta^2}$, and a velocity $\beta = v/c$ where m_0 is the rest mass of the electron and c is the velocity of light. The scattered photon of energy $h\nu'$ goes off at an angle ϕ to the incident direction. The three equations stating conservation of energy and momentum determine everything about the process¹⁸ except the probability for its occurrence.

By quantum mechanical calculations Klein and Nishina¹⁹ have shown that the differential cross section for the number of photons scattered into unit solid angle, at angle ϕ , per electron of material, is given by:

$$\frac{d_e \sigma_t}{d\Omega} = \frac{e^4}{2m_0^2 c^4} \left(\frac{1}{1 + \alpha \text{vers } \phi} \right)^2 \left(1 + \cos^2 \phi + \frac{\alpha^2 \text{vers}^2 \phi}{1 + \alpha \text{vers } \phi} \right) \dots (5.)$$

where $\alpha = h\nu / m_0c^2$ and $\text{vers } \varphi = 1 - \cos \varphi$.

Note that for low energy photons ($\alpha = 0$) equation (5) reduces to the expression for classical scattering, and that for $\varphi = 0$, the recoil electron acquires no energy, and equation (5) reduces to the classical value $e^4/m_0^2c^4$ regardless of photon energy.

In the classical case, $h\nu' = h\nu$ and, therefore, the differential cross section for energy scattered is the same as for the number of photons scattered. In the Compton process, however, the scattered photon acquires a fraction $h\nu' / h\nu = 1 / (1 + \alpha \text{vers } \varphi)$ of the original energy. (As φ increases the photon takes less of the energy, and the electron takes more. This fraction also decreases with increasing energy $h\nu$.) Thus the cross section for energy scattered, is less than the cross section for photons scattered, and is given by:

$$\frac{d_e \sigma_s}{d\Omega} = \frac{1}{1 + \alpha \text{vers } \varphi} \cdot \frac{d_e \sigma_t}{d\Omega} \dots\dots\dots(6.)$$

Multiplying (5) and (6) by $d\Omega = 2\pi \sin \varphi d\varphi$ and integrating from $\varphi = 0$ to $\varphi = 180^\circ$ gives the total Compton absorption coefficient, and the Compton scatter coefficient respectively. Assuming that the energy scattered is not locally absorbed, then the difference between these two coefficients will give the real absorption coefficient

per electron for Compton interactions.

$$e\sigma_a = \int_{\phi=0}^{\phi=180^\circ} (d_e\sigma_t - d_e\sigma_s) \dots\dots\dots (7.)$$

Multiplying $e\sigma_a$ by the electron density gives the Compton linear absorption coefficient, σ_a .

(d) Pair production

The energy associated with an electron at rest is $m_0c^2 = .511$ Mev. At photon energies greater than $2m_0c^2 = 1.02$ Mev., a photon may undergo an interaction with a nucleus in which the photon disappears and an electron and a positron are set in motion with kinetic energy T_+ and T_- . The nucleus acquires an indeterminate amount of momentum but negligible energy. From conservation of energy, $(h\nu - 2m_0c^2) = (T_+ + T_-)$ and T_+ and T_- may vary from zero to $h\nu - 2m_0c^2$. However, the process, except at high energy, will favour $T_+ \approx T_-$.

After the pair have been set in motion, the electron will lose its kinetic energy to the surroundings. The positron will also lose its kinetic energy, and when it has come to rest, or nearly come to rest, it will be annihilated by an electron. When the annihilation occurs the energy, $2m_0c^2$ appears in the form of two photons ejected in opposite directions each with an energy m_0c^2 .

The total cross section per atom for pair production, $\sigma_a K$, may be found by a complicated theoretical analysis.¹⁹ Neglecting the effects of screening, the pair

cross section per atom varies as Z^2 . At high photon energies in elements of large Z , the pair process can occur outside the K shell, and the screening effect reduces the cross section.

Neglecting the energy loss of the pair by bremsstrahlung, the fraction of the initial energy, $h\nu$, which is truly absorbed is $(h\nu - 2m_0c^2)/h\nu$. Thus the real pair absorption coefficient is given by

$$K_a = \frac{K (h\nu - 1.02)}{h\nu} \dots\dots\dots(8.)$$

where $h\nu$ is in Mev.

At times the pair process may occur in the field of an electron, and then two electrons and a positron are set in motion. The threshold energy for this triplet production is $4m_0c^2$, and at high energies the cross section is approximately $1/Z$ of the pair cross section. At lower energies it is a smaller fraction of the pair cross section.

(2) Detection and measurement

(a) Definition of the roentgen

The international unit of x-ray dose was first defined at the Stockholm Congress of Radiology in 1928 thus:

"The roentgen is the quantity of x-radiation which, when the secondary electrons are fully utilized and the wall effect of the chamber is avoided, produces in

one cm³ of atmospheric air at 0°C and 76 cm of mercury pressure such a degree of conductivity that one esu. of charge is measured at saturation current."

This definition was modified at the Chicago Congress of Radiology in 1937, to read:

"The roentgen shall be the quantity of X or gamma radiation such that the associated corpuscular emission per 0.001293 gm. of air produces, in air, ions carrying one esu. of quantity of electricity of either sign."

The roentgen has been redefined in Handbook 84 of the International Commission on Radiological Units and Measurements (I.C.R.U.), report 10-a, 1962, but the meaning is essentially the same. They do, however, emphasize that the roentgen is a unit of radiation exposure and not a unit of absorbed dose.

(b) Absorbed dose

The fundamental unit of absorbed dose is the erg/gm. A more convenient unit is the rad, defined to be an absorbed dose of 100 ergs/gm. Absorbed doses from here on will be expressed in terms of the rad.

If 1 cm.³ of air is exposed to 1 roentgen, a number of ion pairs will be produced whose net charge is 1 esu. Each ion pair contributes $e = 4.8 \times 10^{-10}$ esu.

These ion pairs are produced in 0.001293 gm of air. The average energy required to produce an ion pair in air, W , is a constant, independent of energy above 20 kev., and the best value of W to date is 33.7 ev.²⁰ Thus, since 1 ev = 1.6×10^{-12} ergs, the energy absorbed by one gram of air exposed to one roentgen is

$$\frac{(33.7) (1.6 \times 10^{-12})}{(4.8 \times 10^{-10}) (0.001293)} = 86.9 \text{ ergs}$$

i.e.: air exposed to 1 roentgen will absorb .869 rads.

The energy absorption per roentgen in a medium other than air, may be calculated if the mass absorption coefficient is known, from the formula:

$$E_m = .869 \frac{(u/\rho) \text{ medium}}{(u/\rho) \text{ air}} \text{ rads.} \dots \dots \dots (9.)$$

The factor $(.869 (u/\rho) \text{ medium} / (u/\rho) \text{ air})$ is known as the f factor, and if the medium is water (or tissue) $f = 0.965$ at 1 Mev. ($f = .957$ in muscle, and $.919$ in bone at 1 Mev.) The f factor varies little with energy for tissue or muscle, but increases to 4.39 at 30 kev. in bone due to the large cross section for photoelectric absorption.²¹

(c) Measurement of exposure in roentgens

The apparatus used almost universally to measure x-ray dose in accordance with the definition of the roentgen is an adaptation of the parallel-plate ionization chamber.¹ It is called a "free air" chamber because the secondary

electrons which produce the ionization originate and complete their tracks in the air of the chamber. The field between the electrodes of the ionization chamber must be sufficient to collect all the ions without recombination, but not so high that the moving ions produce further ionization by collision processes. Such chambers are operated by the national standardizing laboratories, and are most accurate for x-rays generated at 50 to 200 kv.

In a "thimble" or cavity ionization chamber conditions are different since the walls of the chamber are irradiated and the ionization of the gas is due to electrons arising from quantum absorption both in the walls and in the gas filling. A homogeneous "air-wall" chamber is not practicable for there is no solid with the same atomic composition as atmospheric air. However, if the cavity has dimensions such that only a very small fraction of the electron energy is lost in crossing it, and such that direct absorption of quantum radiation by the gas in the cavity is negligible, and if it is surrounded by walls thick enough that all electrons entering the cavity originate in the wall, and if the source of quantum radiation is sufficiently far from the cavity for the divergence of the beam to be negligible over the cavity dimensions, then the energy, E , imparted by the electrons

to unit mass of the wall material may be related to the ionization in the gas by

$$E = \frac{S_M}{S_G} J_G W \dots\dots\dots(10.)$$

where J_G is the number of ion pairs formed per unit mass of gas, W is the mean energy expended in the production of a pair of ions in the gas, and S_M and S_G are the mass stopping powers of the wall material and the gas. This is known as the Bragg-Gray relationship.^{22,23,24} Chambers with air volumes 1 or 2 cm. in diameter fulfill the conditions for the Bragg-Gray principle for dosimetry of gamma rays of energies greater than about 1 Mev. Chambers must be much smaller at lower energies, or must be operated at lower gas pressure.

In recent years the Bragg-Gray theory has been modified to express a relationship between ionization and flux of various types of radiation.^{25,26} The simple expression (10) has been modified, and stopping powers have been studied extensively.²⁷ Cavity chambers are calibrated by the national standardizing laboratories, using free air chambers for x-rays below about 300 kv and using internationally calibrated cavity chambers above this energy up to 3 Mev.

B. ELECTRONS

(1) Interaction with matter

Electrons lose energy by a variety of processes, including resonance absorption, collisions with nuclei and electrons, excitation of atoms, radiation production (bremsstrahlung), and electrodisintegration of nuclei. For energetic electrons, collisions which produce ionization and excitation of atoms, and radiation production predominate. The latter results in energetic x-rays which are not locally absorbed, so only ionization and excitation are important as far as energy deposition in the medium is concerned.

The stopping power, per electron of the absorbing material, may be calculated using the Bethe-Bloch formula for the energy loss of β particles in passing through matter:

$$e_s = \frac{2\pi e^4}{m_0 c^2 \beta^2} \left[\ln \frac{m_0 c^2 \beta^2 T}{2 I^2 (1 - \beta^2)} + (1 - \beta^2) - \left(2 \sqrt{1 - \beta^2} - 1 + \beta^2 \right) \ln 2 + \frac{1}{8} \left(1 - \sqrt{1 - \beta^2} \right)^2 - \delta \right] \dots (11.)$$

where e , m_0 , c , and β have their usual significance, I is the average excitation potential of the atom, and T is the kinetic energy of the incident electron. Multiplying e_s by the electron density of the medium gives the energy loss per unit path length, $-dT/dx$, of the incident electron in the medium, due to excitation and ionization of the atoms. The term δ , is included to correct

for the density effect or polarization effect of condensed media.^{19,28,29,30,31,32}

The radiative energy loss of electrons due to negative acceleration has been calculated¹⁹ and an approximate relative magnitude of collision and radiation energy loss is¹⁷

$$\frac{(dT/dx)_{coll.}}{(dT/dx)_{rad.}} = \frac{1600 m_0 c^2}{T Z} \dots\dots\dots(12.)$$

(dT/dx) coll. is due to a large number of small energy losses whereas (dT/dx) rad. is due to a relatively few number of interactions each involving a large energy loss.

(2) Detection and measurement

Detection and measurement of high energy electron beams, and of X or gamma rays above 3 Mev. frequently relies on chemical dosimeters or solid state devices. A standard aqueous system such as the ferrous-ferric dosimeter³³ (radiation induces a change in the relative numbers of these ions) can be calibrated against ionization chambers or calorimeters, or may be calibrated by other indirect methods.³³ This particular system is quite accurate now, but it is insensitive to doses of less than 1000 rads. The thermoluminescence of LiF, as this paper will show, can be a useful tool in electron beam dosimetry, and it is sensitive to much smaller doses.

CHAPTER III

THERMOLUMINESCENCE IN LITHIUM FLUORIDE

Before considering the nature of the trapping centers in LiF it is necessary to discuss briefly a few important concepts of the solid state.

A. ENERGY BANDS, TRAPS, AND GLOW CURVES

(1) Band theory applied to LiF

The atomic electrons of a single atom exist in discrete energy levels, separated by large forbidden energy regions. A similar situation exists in a solid except that the single levels widen into energy bands due to interactions between the atoms in the crystal. These bands of allowed energies are separated by forbidden regions. In LiF, the 2s level of Li forms the uppermost band, the conduction band, but in the ionic crystal these electrons are transferred to fluorine, and the conduction band is empty. The 2p level of fluorine forms the next band, the valence band, and in the ionic crystal this band is full. All lower bands are full.

(2) Trapping levels

Even a pure crystal cannot exist as a perfect crystal. For thermodynamic equilibrium there must be a certain number of ion vacancies distributed randomly throughout the crystal.

If the crystal is not pure there will be impurity atoms also distributed throughout the crystal. Electrons occupying positions at one of these impurity atoms or vacancies may have energies which would be forbidden in the perfect crystal, and hence may lie between the valence and conduction bands.

Electrons may be excited from the valence to the conduction band by ionizing radiation. These electrons can travel through the crystal, and some of them will drop into the localized levels created by the crystal defects. If the transition from there to the valence band is forbidden, the electron remains trapped - until it is thermally excited out of the trap into the conduction band, from where it can de-excite back to the valence band with the emission of light.

(see Fig. 1.)

The electron in the trap has a mean lifetime τ , which depends on the trap depth and on the temperature. If P is the probability of liberating a trapped electron, per second, then $P = 1/\tau$ and

$$1/\tau = P = S e^{-E/kT} \dots\dots\dots (13.)$$

where E is the trap depth, T the absolute temperature, and S is a frequency which gives the number of times per second that the electron hits the barrier.³⁴

(3) Glow curves or thermoluminescence curves

After the traps have been filled by irradiation, the solid is warmed at a uniform rate, B . The traps empty as the

temperature rises, the "shallow" ones first, and at each temperature T those with lifetimes of a fraction of a second or so are principally responsible for the observed thermoluminescence. If there is only one trap depth the thermoluminescence is very weak initially, then increases with T , reaches a maximum for the temperature of thermoluminescence, T^* , and then decreases to zero as the traps are all emptied. The resulting curve of light intensity vs. time (or temperature) is called a glow curve. Knowing T^* it is possible to calculate the trap depth E from the following theory of Randall and Wilkins^{34,35}

If n is the number of filled traps at time t , and if τ is the mean lifetime of the trapped electrons, then

$$\frac{dn}{n} = - \frac{1}{\tau} dt \dots\dots\dots(14.)$$

or $n = n_0 e^{-t/\tau} \dots\dots\dots(15.)$

The thermoluminescence intensity I is given by:

$$I = \left| \frac{dn}{dt} \right| = \frac{n}{\tau} \dots\dots\dots(16.)$$

Now, if the temperature, T , is allowed to increase with time according to $dT = B dt$, and if τ varies according to (13), then (15) must be replaced by:

$$n = n_0 e^{-\int_0^t \left(\frac{dt}{\tau(t)} \right)} = n_0 e^{-\int_{T_i}^T \left(s e^{-E/kT} \frac{dT}{B} \right)} \dots\dots\dots(17.)$$

and the thermoluminescence intensity $I(T)$ at the temperature T is given by

$$I(T) = n_0 S e^{-E/kT} - \int_{T_i}^T \left(S e^{-E/kT} \frac{dT}{B} \right) \dots \dots \dots (18.)$$

The trap depth E may be found from T^* by setting $(dI/dT) = 0$ at $T = T^*$. This gives

$$\frac{BE}{k(T^*)^2} = S e^{-E/kT^*} \dots \dots \dots (19.)$$

The need to know S can be avoided by using two different warming rates B_1 and B_2 . The same trap depth then results in two different temperatures for the peak in the glow curve T_1^* and T_2^* . Thus S can be eliminated from (19) to give

$$\frac{E}{k} \left(\frac{1}{T_2^*} - \frac{1}{T_1^*} \right) = \ln \left(\frac{B_1 (T_2^*)^2}{B_2 (T_1^*)^2} \right) \dots \dots \dots (20.)$$

from which E is easily obtained. Since T^* varies very little with warming rate, E can only be estimated with a 20 or 30% accuracy.³⁵

B. TRAPPING CENTERS IN LITHIUM FLUORIDE

The mechanism of thermoluminescence and the nature of the traps in LiF is not accurately known. Most investigations published recently are concerned with the application of the thermoluminescence rather than with its mechanism. It is known, however, that ionizing radiation causes the production of F-centers in LiF. An F-center is an electron trapped in a negative ion vacancy, and the radiation not only fills existing

negative ion vacancies with electrons, but also creates additional vacancies. Alpha particles have enough momentum to displace lattice ions thus creating vacancies and F-centers all along their range. Gamma rays or electrons with their small momentum can produce vacancies only at dislocations where binding energies are reduced.⁶ F-centers are detected easily because the electron can be excited from its ground state (about 5 ev. below the bottom of the conduction band) to a level just below the conduction band by light of about 2500 Å. Morehead and Daniels⁶ have shown that this F-band absorption is related directly to the total amount of thermoluminescence (as determined from the area under a glow curve). This indicates that all of the thermoluminescence is related to the emptying of F-centers as the crystals are heated.

Positive ion vacancies are also found in LiF, and the ionizing radiation creates more of these. One of the surrounding negative ions will then tend to give away an electron. Since the six surrounding ions will tend to share the loss, the resulting "hole" will be associated with the positive ion vacancy; the combination of vacancy and hole is called a V-center. Other types of more complicated centers involving more than one vacancy will also be formed.

Morehead and Daniels also refer to transition centers which can capture an electron from the conduction band

and return it to the valence band, in some cases by radiation of light. The de-excitation may be due to the recombination of electrons from F-centers with holes from V-centers, the transition centers being the stepping stone. As the temperature is raised the number of empty traps increases, and the supply of transition centers diminishes. "Once this supply has been exhausted further light emission from the emptying of F-centers must wait until a higher temperature is reached when more holes are released from V-centers to re-activate the transition centers. The escape of an electron from an F-center remains the rate determining step and hence the activation energy of the F-center is greater than that of any V-center."⁶

CHAPTER IV

APPARATUS AND PRELIMINARY OBSERVATIONS

The thermoluminescent dosimeter (TLD) was purchased from Controls for Radiation Inc. (Con-Rad.) It is a complete dosimetry system based on the thermoluminescence of LiF. Preliminary results with this system were encouraging.

A. APPARATUS

The Con-Rad system consists of LiF phosphor, ground into a crystalline powder, two sieves for selecting only crystals within a certain size range, an aluminum dispenser which dispenses a constant amount of phosphor, polyethylene capsules in which the LiF is irradiated, a readout instrument which heats the irradiated phosphor, and measures the amount of light emitted, metal planchets which hold the phosphor for insertion into the readout instrument, and a self luminous light source for calibration purposes.

The LiF powder is classified as type-N or type-7 as described earlier. All measurements were made with type-N unless otherwise stated.

The phosphor dispenser is a volumetric device which dispenses about 60 mg. of powder (Fig. 2.) The phosphor to

FIGURE 2.

APPARATUS



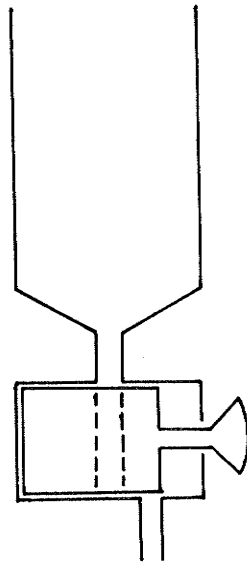
CAPSULE AND CAP

(actual size)



PLANCHET

(actual size)



PHOSPHOR DISPENSER

be used is placed in the cylindrical hopper. The slide is pushed in and then pulled out to dispense the proper amount of powder.

When the planchet containing the powder is inserted into the readout instrument, it is gripped by a pair of copper fingers. When the start bar on the front of the instrument is depressed, a current of about 150 amps. flows through the planchet for 10 seconds, heating the planchet to about 300°C. An EMI 9536 S photomultiplier tube is seated 1.4 cm. above the planchet, and at the moment the start bar is depressed its output is connected to a 10 uf polystyrene capacitor. An electrometer tube of input resistance 10^{10} ohms, connected as a cathode follower, is used to measure the voltage on the integrating capacitor. The output of the electrometer is displayed on a digital voltmeter with a 100 mv (1000 digits) full-scale sensitivity. The integrating capacitor remains connected to the photomultiplier for 15 seconds, after which time the integrated response is read. When a second sample is inserted, and the start bar is depressed, the capacitor is momentarily shorted erasing the previous reading. There was no response on the instrument when an empty planchet was put through a heating cycle.

A zero adjustment and a calibration adjustment are provided. To extend the range of measurements a scale switch is also provided. When this is depressed, a 90 uf capacitor is momentarily connected in parallel with the 10 uf integrating

capacitor draining 9/10 of its charge. The voltmeter reading is thus reduced by a factor of 10 each time the scale switch is pressed.

A variac is provided in the primary of the heater circuit to adjust the current through the planchet, and a voltmeter connected across the copper fingers measures the voltage drop across the planchet.

It was found necessary to install additional apparatus, especially for trouble shooting. An ammeter was installed in the secondary of the heater circuit so that the total power developed in the planchet could be calculated. Thermocouples were silver soldered to the bottom of a few planchets, and heating curves were obtained by feeding the voltage developed into a recorder. A thermocouple was also installed in the photomultiplier housing, near the photocathode. A microammeter was installed to measure the output current of the photomultiplier tube.

B. PRELIMINARY OBSERVATIONS

(1.) Digital voltmeter

It was found that the digital voltmeter did not run smoothly, but rather it moved in short pulses of about 0.05 mv (0.5 digits.) For example, a series of readings with the standard light source would give 101.2 digits or 101.8 digits but never anything in-between. The voltmeter was calibrated with a

standard cell and a voltage divider. The total error was found to be less than 2% at 1.5 mv (15 digits) and less than 0.2% at 100 mv (1000 digits.)

(2.) Phosphor dispenser

After four months of use the average weight of twenty samples of LiF from the dispenser was 59.7 mg. with a standard deviation of 0.6%. After 10 months of use the average sample weight was 60.1 mg. and after 20 months it was 61.5 mg. with the same batch of powder. The standard deviation remained about the same. However, at the end of the 20 month period the average sample weight using a new batch of powder was 58.6 mg. Therefore, the increase in sample weight cannot be attributed to wear of the dispenser, but rather to a change in the phosphor. (Under a microscope the new crystals were transparent and had very jagged edges. The old crystals were duller, and the edges were somewhat smoother. This would allow them to be packed closer together in the dispenser.)

(3.) Response to 100 roentgens

The standard deviation of the response of twenty samples of powder, exposed to 100 roentgens, was found to be less than 2%. An attempt was made to correlate fluctuations in response with fluctuations in sample weight, or with fluctuations in planchet current, but no correlation was found. An attempt was made to improve the results by allowing a cooling time of 2 minutes between read-

ings. (This is recommended in the Con-Rad manual.) No virtue was found in this when only a few (twenty) readings were being taken. (It was found in later experiments, however, that this cooling time should be allowed when a few hundred readings are being taken during the day.)

(4.) Powder distribution in the planchet

The technique used is to tip the powder from the capsule into the planchet by hand, and then to drop the planchet lightly a few times to roughly level the powder. The response was found to be a maximum with the powder as level as possible. If the powder was slightly (but noticeably) heaped in the middle or around the edges of the planchet the response was decreased by 2 or 3%. If the planchet was deliberately dropped lightly many times, the powder tended to heap around the edges leaving no powder in the center of the planchet. This resulted in readings 8-12% low. If no attempt was made to level the powder after being spilled from the capsule, the response was found to be as much as 50% low.

These results show that the distribution of the powder in the pan portion of the planchet is the most likely source of random error in the measured response. However, careful visual inspection can assure proper leveling and minimize this source of error.

Various amounts of powder from 10 mg. to 120 mg. were read-out and it was found that the response was nearly proportional to the amount of powder in the planchet. The response/mg. was 11% lower at 120 mg. than it was at 10 mg. due to the increased number of layers of powder (powder was only one layer deep at 10 mg.) This indicates insufficient heating of the top layer, or scattering of the light from the bottom layers by the top layers, or both, when the powder is too deep. With one year old powder that was noticeably yellowed, the response/mg. was 35% lower at 120 mg. than it was at 10 mg. indicating an increased scattering of light from the bottom layers.

(5.) Power requirements to planchet

The power delivered to the planchet must be sufficient to heat the powder to a high enough temperature and to hold it there for a long enough time to release all the trapped electrons. If the temperature becomes too high, however, a high temperature thermoluminescence caused by previous mechanical shaking will be emitted. (tribothermoluminescence.) With a Con-Rad D-15 stainless steel planchet 70 watts was the minimum requirement to release all the energy from the phosphor. With the variac at its maximum setting the power was about 72 watts and no tribothermoluminescence was observed. The variac was left at its maximum. When the planchets had been used several times their surfaces became

dull, heat losses were increased, and 72 watts was no longer sufficient. The planchets were then discarded. Con-Rad D-20 planchets showed greater heat losses and sufficient power could not be supplied to them. Therefore D-15's were used in all experiments.

CHAPTER V

EXPERIMENTAL METHODS AND RESULTS

Some of the experiments described below pertain only to clinical measurements with the particular system under investigation. Other experiments are of a more general nature and were performed in order to gain a better understanding of thermoluminescence in LiF.

A. CALIBRATION CURVES

In all measurements, five capsules of LiF were exposed simultaneously in a tissue equivalent phantom. The phantom was prepared by sandwiching a perspex slab between sheets of a special tissue equivalent rubber. A hole, 3 cm. in diameter, was drilled from one edge of the perspex slab into the center of the phantom. A hollow perspex cylinder, 3 cm. in diameter, was filled with paraffin and five small holes were drilled in the side of the cylinder near one end. The five capsules were then placed in these holes and the cylinder was fitted into the hole provided in the phantom. The rubber, perspex, and paraffin, the polyethylene capsules, and even the LiF itself are all nearly tissue equivalent materials as far as absorption of radiation is concerned.



Other cylinders were shaped to house various ionization chambers and one was shaped to hold a plastic test tube containing ferrous sulphate solution. Thus, each of these dosimeters could be exposed at the same point in the phantom. (but not at the same time.)

The radiation (x-rays, gamma rays, or electrons) was then allowed to fall normally onto the rubber surface of the phantom. The distance of the dosimeter from the surface was varied by changing the number of sheets of rubber in front of the perspex slab.

(1.) Cobalt calibration

The cobalt exposures were made on an A.E.C.L. Theratron, model F, with a 10 x 10 cm. field at 75 cm. from the source to the surface of the phantom. Six cm. of rubber in front of the perspex slab placed the center of the dosimeter at a depth in the phantom equivalent to 7.9 cm. of water. A sub-standard ion chamber, calibrated by N.R.C., was used to measure the exposure rate (roentgens/min.) at that point in the phantom. The exposure rate was then multiplied by the f factor (see page 23) for water at 1 Mev.* to give the number

* The f factor used above was 0.974 and was based on

$W = 34 \text{ ev.}^{36}$ This was revised in 1963 to 0.965 based on

$W = 33.7 \text{ ev.}^{21}$, however, the calibration was completed

prior to receipt of the revised f factor and the necessary correction was not applied.

of rads per minute that would be absorbed by water (or tissue) if it were exposed at that point in the phantom.* A timer which operates the shutters of the teletherapy unit was then set to give the desired number of "rads". Then LiF capsules were exposed, five at a time, to various doses and the average TLD response was plotted as a function of absorbed dose. i.e.: as a function of rads absorbed in water.

This calibration curve is shown in Fig. 3. The curve is not linear, and it is therefore impossible to calibrate the instrument to read 1 digit = 1 rad. except over a very small range. The curve is similar in shape to those presented by Cameron et al¹¹, Karzmark et al¹⁴, and Marrone and Attix.¹⁵ The departure from linearity is shown effectively in Fig. 4.

* In choosing the f factor for 1 Mev. gamma rays, scattered radiation has been ignored. Singly scattered photons probably account for less than 20% of the total beam intensity, and have an energy spectrum peaked at about 300 kev.^{37,38} Multiply scattered photons would have lower energy but would account for less than 2% of the total beam intensity.³⁷ Also, the f factor for water varies by less than 10% over the range from 10 kev to 1 Mev.²¹

FIGURE 3.

CO^{60} CALIBRATION

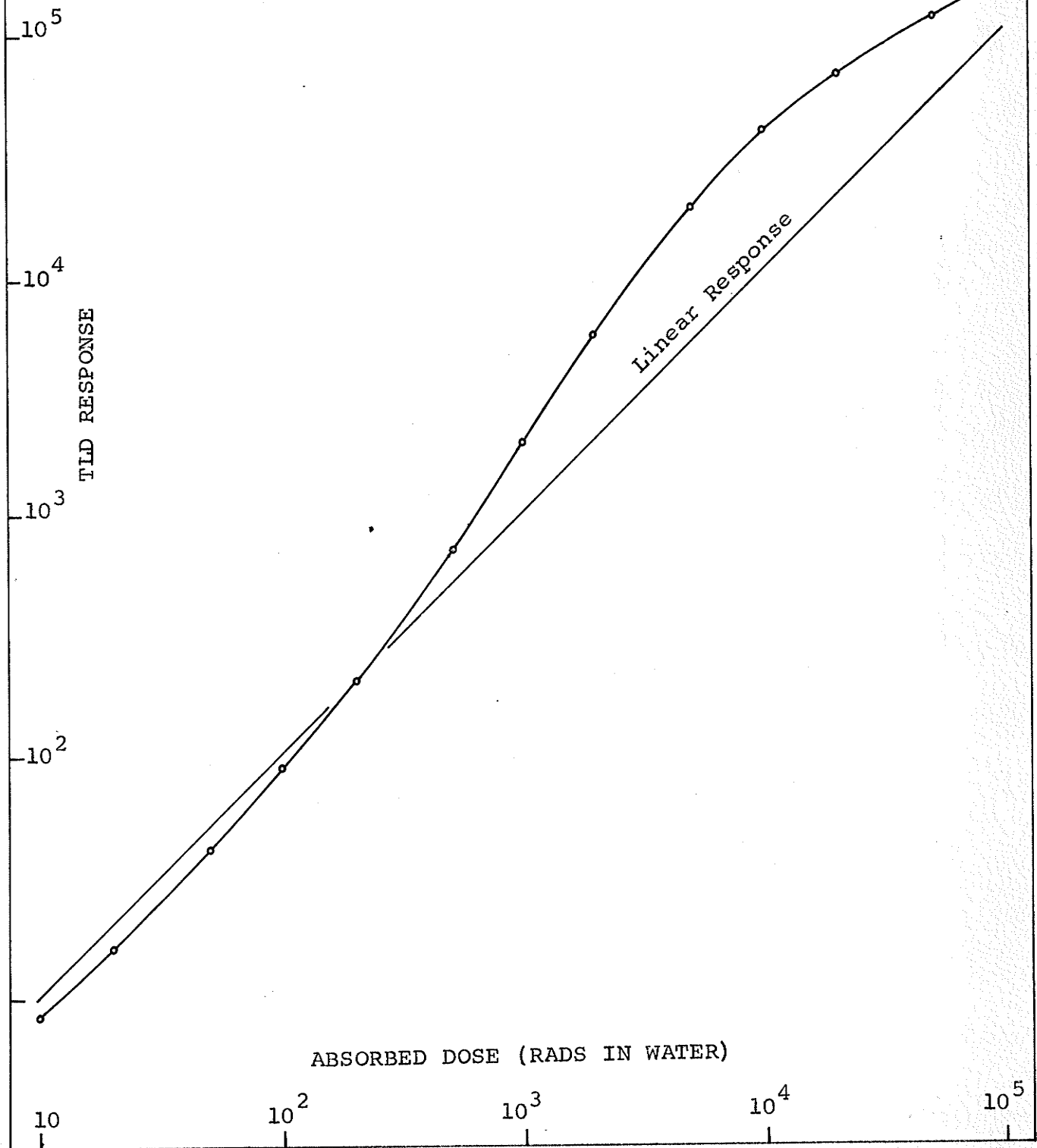
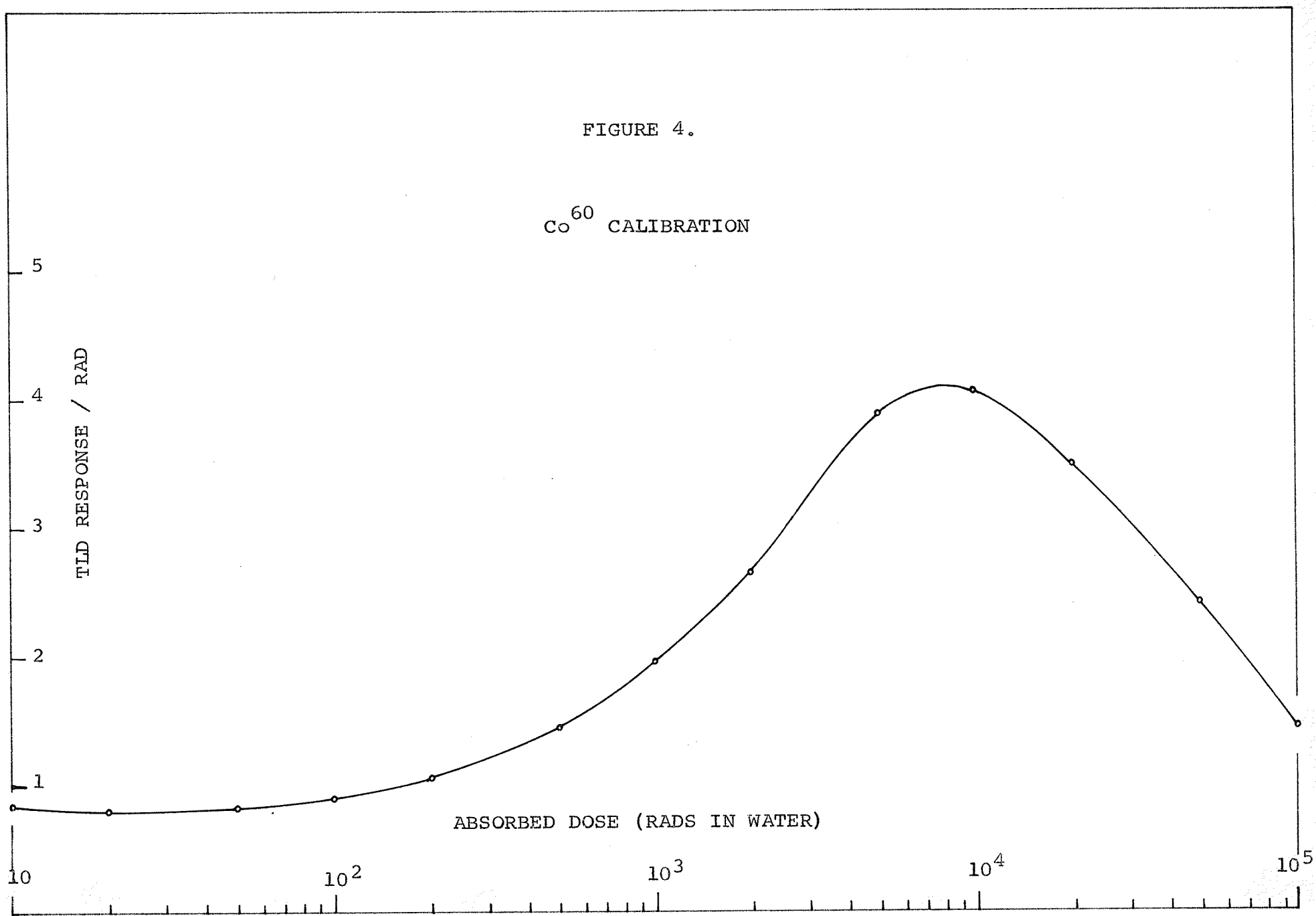


FIGURE 4.

Co^{60} CALIBRATION



where response per rad is plotted vs. rads. A possible explanation for the increase in response/rad up to 10^4 rads is as follows: If the ionizing radiation creates F-centers by filling vacancies with electrons, and if the radiation also creates vacancies, and if the rate of vacancy creation exceeds the rate of conversion to F-centers, then towards the end of a long exposure there would be more vacancies available for conversion to F-centers, and hence a larger response per rad than at the beginning of the exposure. The fact that the curve turns over around 10^4 rads could then be explained as a saturation of the potential vacancies (such as the atoms near a dislocation edge.) Once no more vacancies were created, the existing ones would be converted to F-centers, and further exposure would not increase the response. This appears to be happening around 10^5 rads (Fig. 3.) The turning over of the response curve could also be the result of permanent damage to the crystals of LiF by high doses. (Such permanent damage was observed and is reported later.)

It is not certain that the response/rad curve turns up at the low doses end, as shown. It has since been found that, due to finite shutter speed and/or timer inaccuracy at small exposure times, the point at 10 rads is 4-5% high and that at 20 rads is 1-2% high. This would flatten the curve at the low dose end.

(2.) X-ray calibration

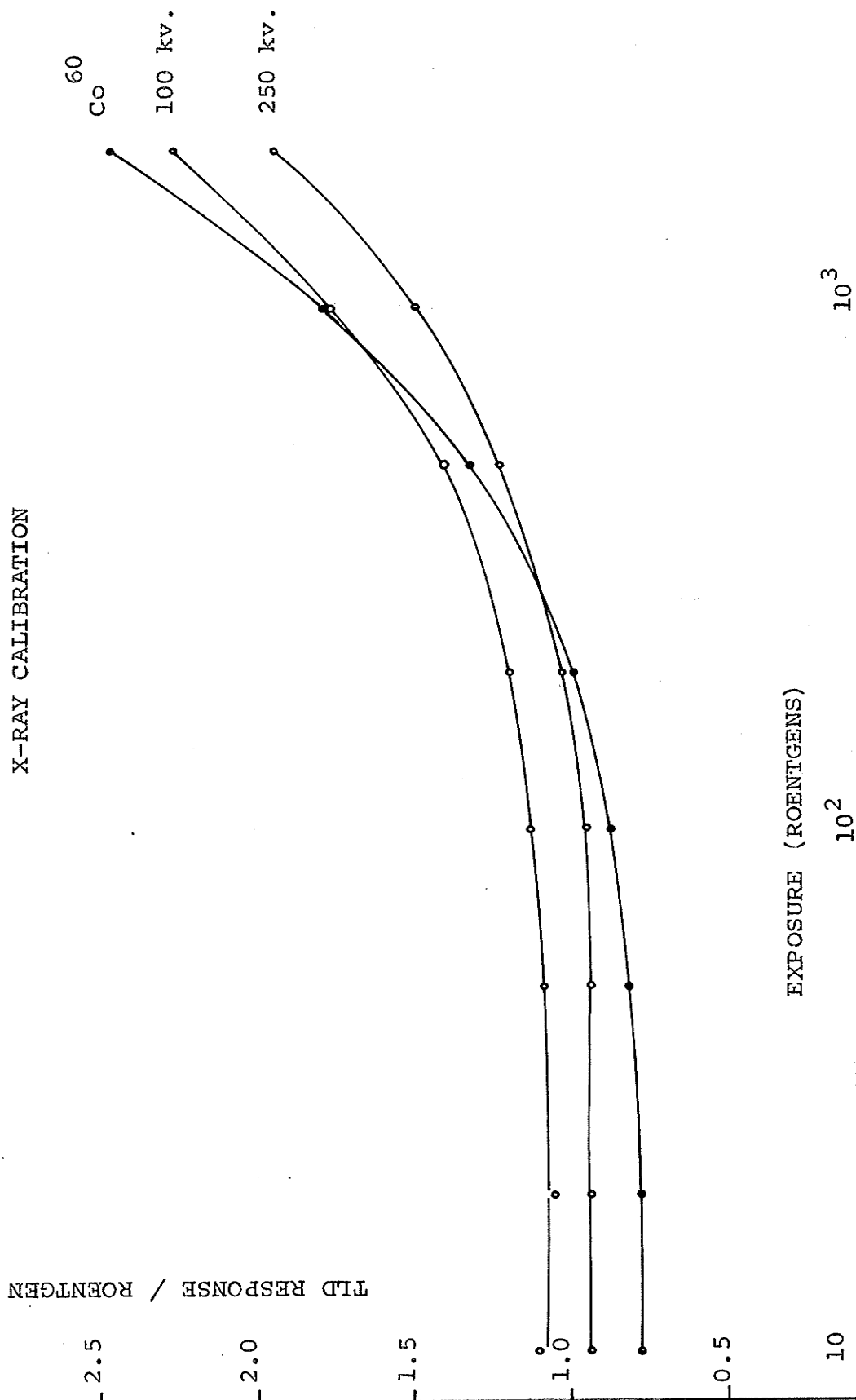
The x-ray exposures were done using a Siemens 250 kv. constant potential x-ray machine. All exposures were made in the phantom with a 10 x 10 cm. field. Calibrations were done for two different tube potentials, 250 kv. with a thoraues filter, H.V.L. (half-value layer)= 2.8 mm. Cu, and 100 kv. with no filter, H.V.L.= 2.5 mm. Al. (These are the standard energies used in treatment of patients.) The higher energy exposures were done at a depth equivalent to 3.8 cm. of water and the lower energy ones at 1.7 cm. of water. Exposure rate was measured as for cobalt.

In Fig. 5 the TLD response per roentgen is plotted vs. roentgens for both x-ray energies and also for Co^{60} . It is seen that the shapes of the curves are different than for Co^{60} . A possible explanation is that the lower energy x-rays could not create vacancies as easily as the higher energy gamma rays, but the x-rays could fill the vacancies with electrons just as the gamma rays do. A smaller vacancy production would result in a less pronounced increase in response per roentgen with increasing exposure time.

Cameron et al^{8,10,11} have reported that the response to 30 kev. effective x-rays is 30-40% greater than the response to Co^{60} (due to the increase in the f factor for LiF at low energy.) According to Fig. 5 this is true only for exposures

FIGURE 5.

X-RAY CALIBRATION



of less than 100 roentgens, (the energy spectrum at 100 kv. could be likened to what Cameron calls 30 kev. effective x-rays) and at exposures around 1000 roentgens the LiF is less sensitive to the soft x-rays than to the Co^{60} gamma rays.

The response of the LiF to x-rays, relative to Co^{60} is shown as a function of exposure in Fig. 6.

(3.) Electron calibration

The electron exposures were done using a 35 Mev. betatron, constructed and installed by Brown-Boveri. The electrons pass through an ion chamber on their way out of the betatron, and when the ionization builds up to a certain level, a counter is triggered. The dose delivered is determined by the number of "kicks" registered on the counter.

All exposures were made in the phantom at a depth equivalent to 1.7 cm. of water. An aqueous solution of ferrous sulphate was placed in the phantom, and exposed to 3500 "kicks" (approx. 4000 rads) to determine the number of rads per "kick" absorbed by the water. Capsules of LiF were then exposed to various numbers of "kicks" from 10 to 2000. Fig. 7 is a plot of response/rad vs. rads. for two different electron energies, 25 Mev. and 35 Mev. These are compared to a similar curve for Co^{60} gamma rays. (This cobalt curve is the same as that in Fig. 5 except that roentgens have been converted to rads using the f factor for water, 0.965.) The response per rad rises more sharply for the higher energy electrons as would be

FIGURE 6.

X-RAY RESPONSE RELATIVE TO Co^{60}

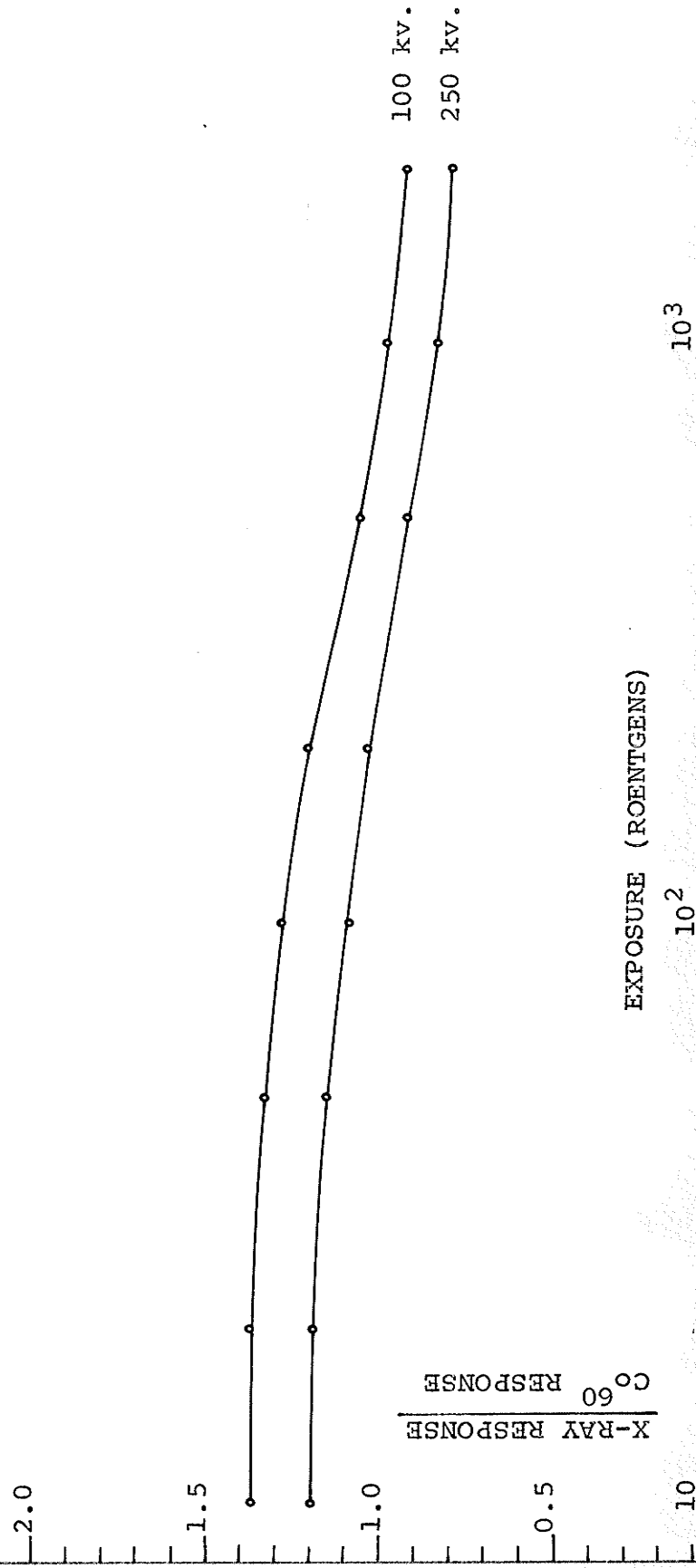


FIGURE 7.

ELECTRON CALIBRATION

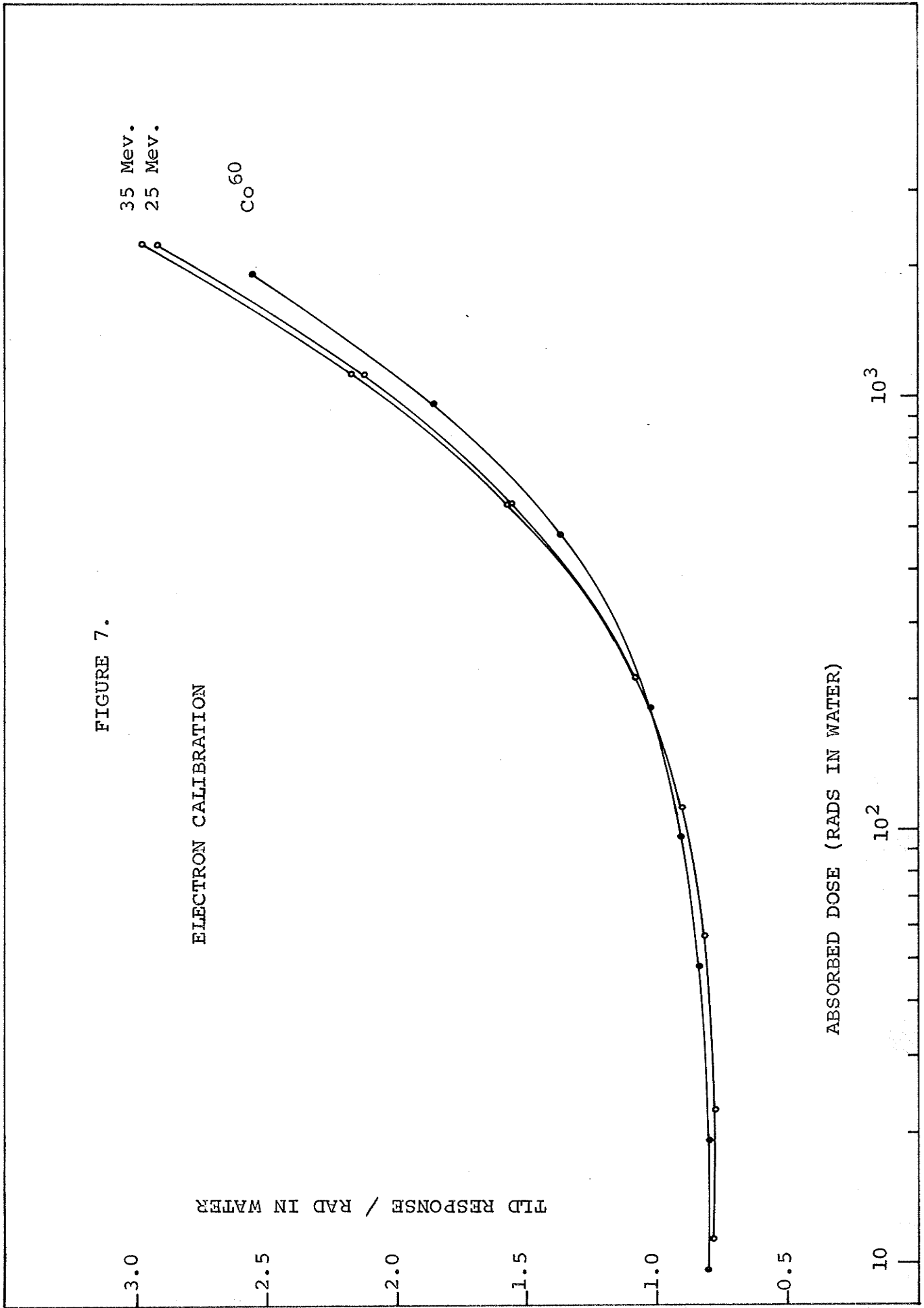
35 Mev.
25 Mev.

Co^{60}

TLD RESPONSE / RAD IN WATER

ABSORBED DOSE (RADS IN WATER)

3.0
2.5
2.0
1.5
1.0
0.5
10²
10³



expected on the model proposed in the last section.

For all three curves shown in Fig. 7 the response is a measure of absorbed dose in LiF, and the dose (in rads) is a measure of absorbed energy in water or tissue. The curves are therefore useful for measuring absorbed dose in tissue, but it may be unrealistic to compare the response curves unless the term "rads" refers to absorbed dose in LiF. Absorbed dose in water was converted to absorbed dose in LiF as follows.

The absorbed dose in water for Co^{60} gamma rays was multiplied by the ratio $(\mu/\rho)_{\text{LiF}} / (\mu/\rho)_{\text{H}_2\text{O}}$ to give the absorbed dose in LiF. This ratio was found to be 0.833 (details of the calculation are in Appendix A.) This assumes that all the electrons responsible for ionization in the LiF were released in the LiF. This is only valid if the volume of LiF is such that its linear dimensions are large compared to the range of a secondary electron. The average range of secondary electrons from Co^{60} gamma rays is 3-4 mm. in water (density = 1) and therefore would be 1-2 mm. in LiF (density = 2.6). The inside diameter of the capsules is 3 mm. and the walls are 1 mm. thick. Therefore, some of the ionization in the LiF is due to secondary electrons generated in the polyethylene walls and in the paraffin.

To determine the extent of the wall effect, the wall was eliminated by irradiating a large volume of LiF, and then reading out dispensed samples of the irradiated powder. The

response was found to be 1.6% higher than for LiF irradiated in capsules, indicating that the effective absorption coefficient (which should be used in place of $(\mu/\rho)_{\text{LiF}}$) is 1.6% lower than that for LiF.

Thus the conversion factor to use in converting absorbed doses from water to LiF for Co^{60} gamma rays is

$$\frac{(\mu/\rho)_{\text{eff}}}{(\mu/\rho)_{\text{H}_2\text{O}}} = 0.820 \dots\dots\dots(21.)$$

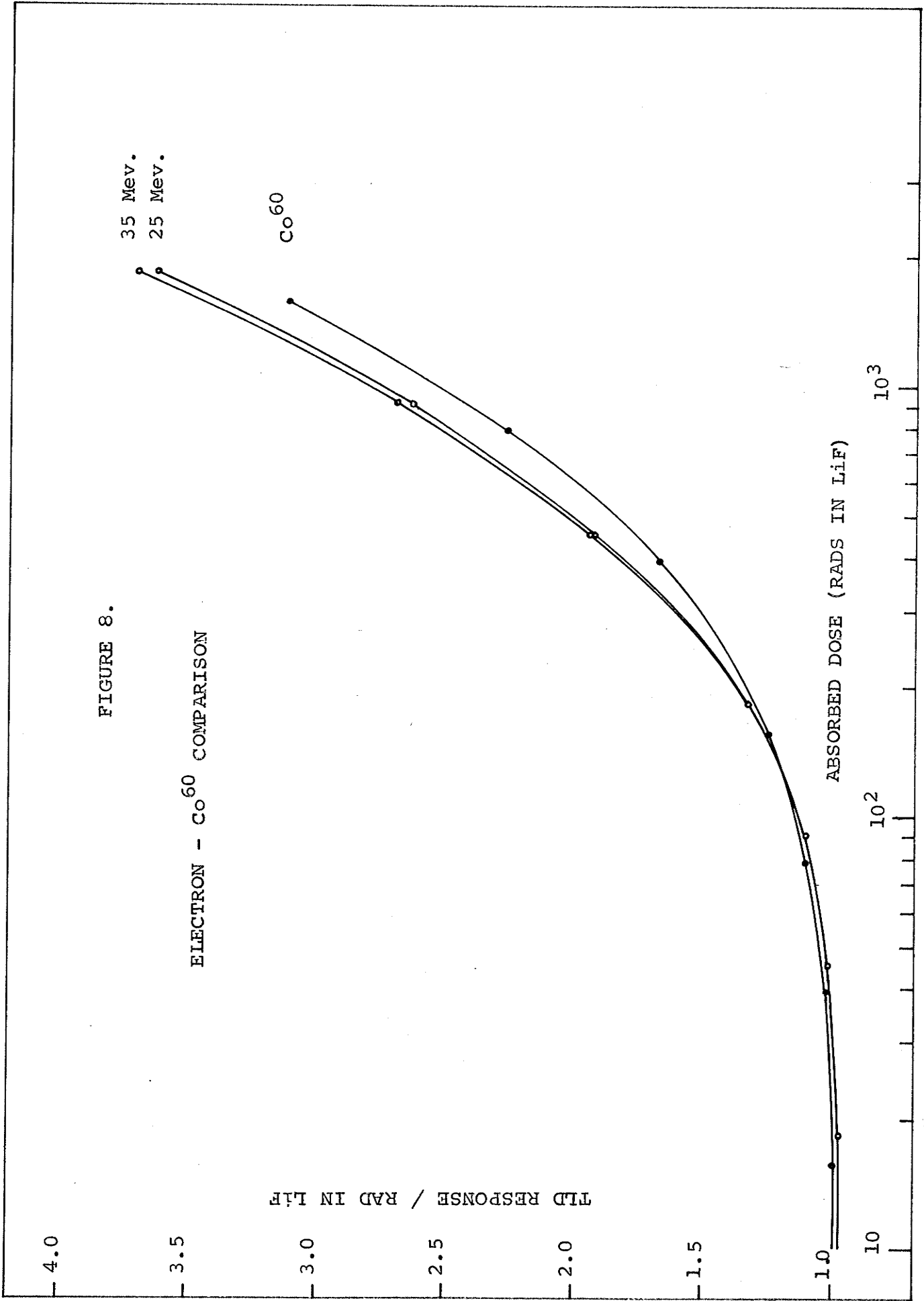
In the case of high energy electrons it is the mass stopping powers which are important, rather than mass absorption coefficients as for electromagnetic radiation. To convert absorbed dose in water to absorbed dose in LiF for the electron beam, the multiplying factor is $(mS)_{\text{LiF}} / (mS)_{\text{H}_2\text{O}}$. The stopping powers are energy dependent, and hence the ratio of stopping powers is also dependent on electron energy. This ratio was calculated (details in Appendix B) from 0.2 Mev. to 50 Mev. and found to vary very little with energy. The ratio was a maximum (0.809) at 10 Mev., and a minimum (0.806) at 0.2 Mev. Ignoring the slight energy dependence, the factor to use for converting absorbed doses from water to LiF for the electron beam is

$$\frac{(mS)_{\text{LiF}}}{(mS)_{\text{H}_2\text{O}}} = 0.808 \dots\dots\dots(22.)$$

In Fig. 8 the data of Fig. 7 is reproduced, but the dose refers to energy absorbed in LiF instead of in water. For

FIGURE 8.

ELECTRON - Co^{60} COMPARISON



low doses, the response/rad is independent of energy, but the energy dependence is appreciable at higher doses. On the previously described model this would be due to the greater ability of the high energy electrons to produce new trapping centers.

At low doses, the ratio of energy absorbed in LiF to energy absorbed in water is the same for the electron beam as it is for Co⁶⁰ radiation, (within 2%) so that powder calibrated with Co⁶⁰ radiation may be used with electrons for routine clinical measurements.

B. STATISTICAL ANALYSIS

It has already been stated that the standard procedure in measuring a dose was to irradiate five capsules of LiF simultaneously and average the readings. In all cases, before reading out the energy, a reading was taken with the standard light source. Then the five samples were read out, followed by another standard light source reading. The standard light source readings were averaged, and the average of the five capsules was then corrected to a standard light source reading of 100.

Standard light source readings were usually between 90 and 110, but could drift downward as much as 6% during one day. If left unused for 2 or 3 hours the instrument would normally recover. It was suspected that the standard light

source may not be fully compensating for the sensitivity drift, and so the following investigation was carried out.

One hundred capsules of LiF were all dosed to 100 rads.(cobalt radiation.) Each was read out in the read-out instrument. At the beginning and after every fifth capsule a standard light source reading was taken. This affected a division of the population of 100 capsules into 20 samples, each sample containing 5 capsules. Each reading in a sample was then corrected for sensitivity drift, the correction factor being determined from the average of the standard light source readings preceding and following the sample.

The sample averages were obtained as well as the standard deviation within each sample. The population average and the standard deviation of the population were also calculated. On the average, the standard deviation, σ , within any sample was 1.08% but σ for the population was 1.25%. In a purely random population these two should be the same, hence in this population there must be an additional between-sample variation. This is also supported by the fact that in a purely random population, the standard deviation of the sample averages should be $(1.25\%)/\sqrt{5} = 0.56\%$ while for this population this figure was 0.81%.

An analysis of variation was carried out by a method described by M. J. Moroney³⁹, to determine the extent

of the between sample variation. The results are summarized in the following table, along with the results of a similar analysis on powder dosed to 1000 rads.

Standard Deviation

<u>Dose</u>	<u>population</u>	<u>within sample</u>	<u>between sample</u>
100 rads	1.25%	1.08%	1.81%
1000 rads	1.74%	1.55%	2.38%

The standard deviation due to the between sample variation is shown in the last column, and was obtained by replacing each member of a sample by the sample average in order to eliminate the within sample variations. It is readily seen that the standard deviation of the readings within a sample is an underestimate of the possible error involved.

In Fig. 9-a the corrected sample averages at 100 rads were plotted as a function of the standard light source reading. During the day the standard light source reading drifted down from 104 to 99, a change of 5%. The sample averages, even after being corrected, show a downward drift of about 2%, indicating that the standard light source was not correcting adequately for the drift. At 1000 rads where the drift might be expected to be larger, it was in fact smaller. The standard light source only drifted by 2%, and the sample averages did not show the strong functional dependence on the standard light source reading, although there was still considerable spread in sample averages. (Fig. 9-b)

FIGURE 9-A.

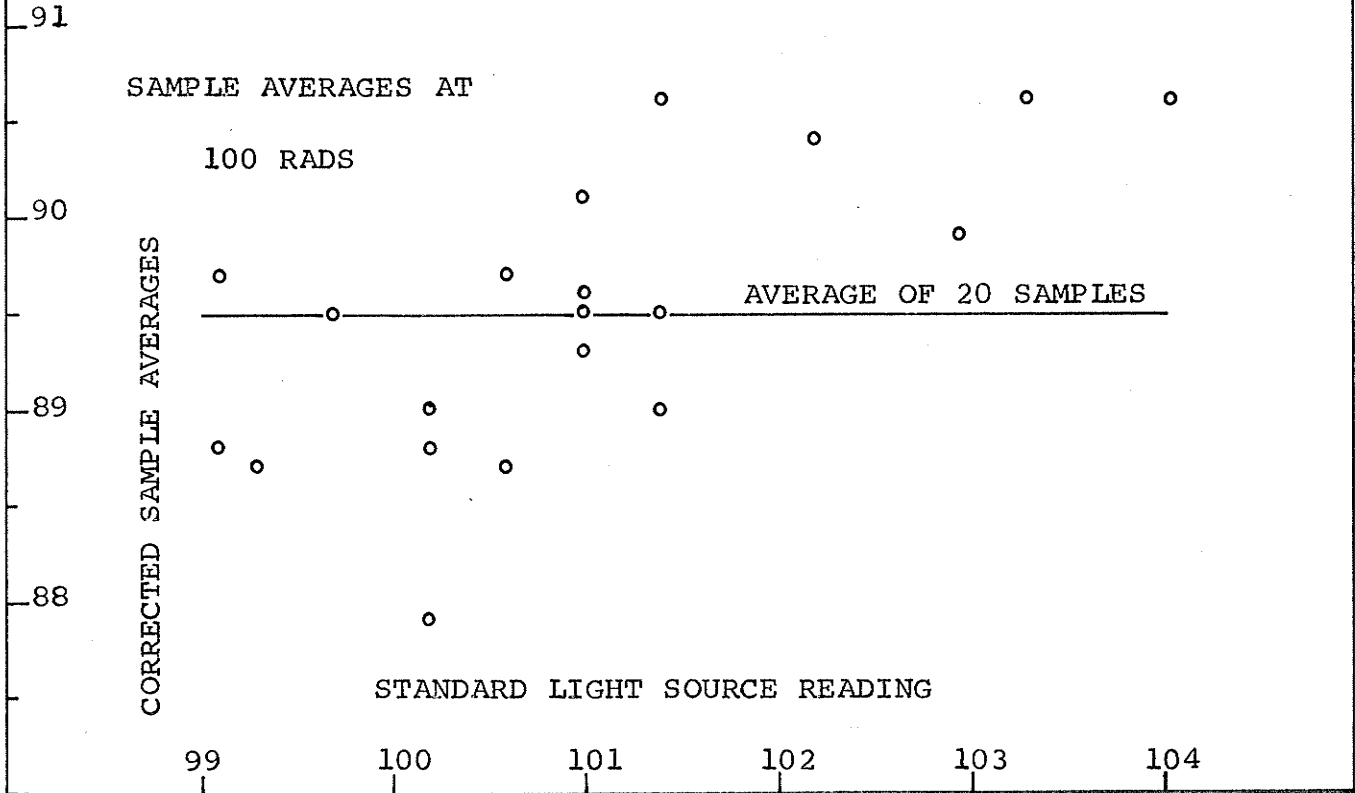
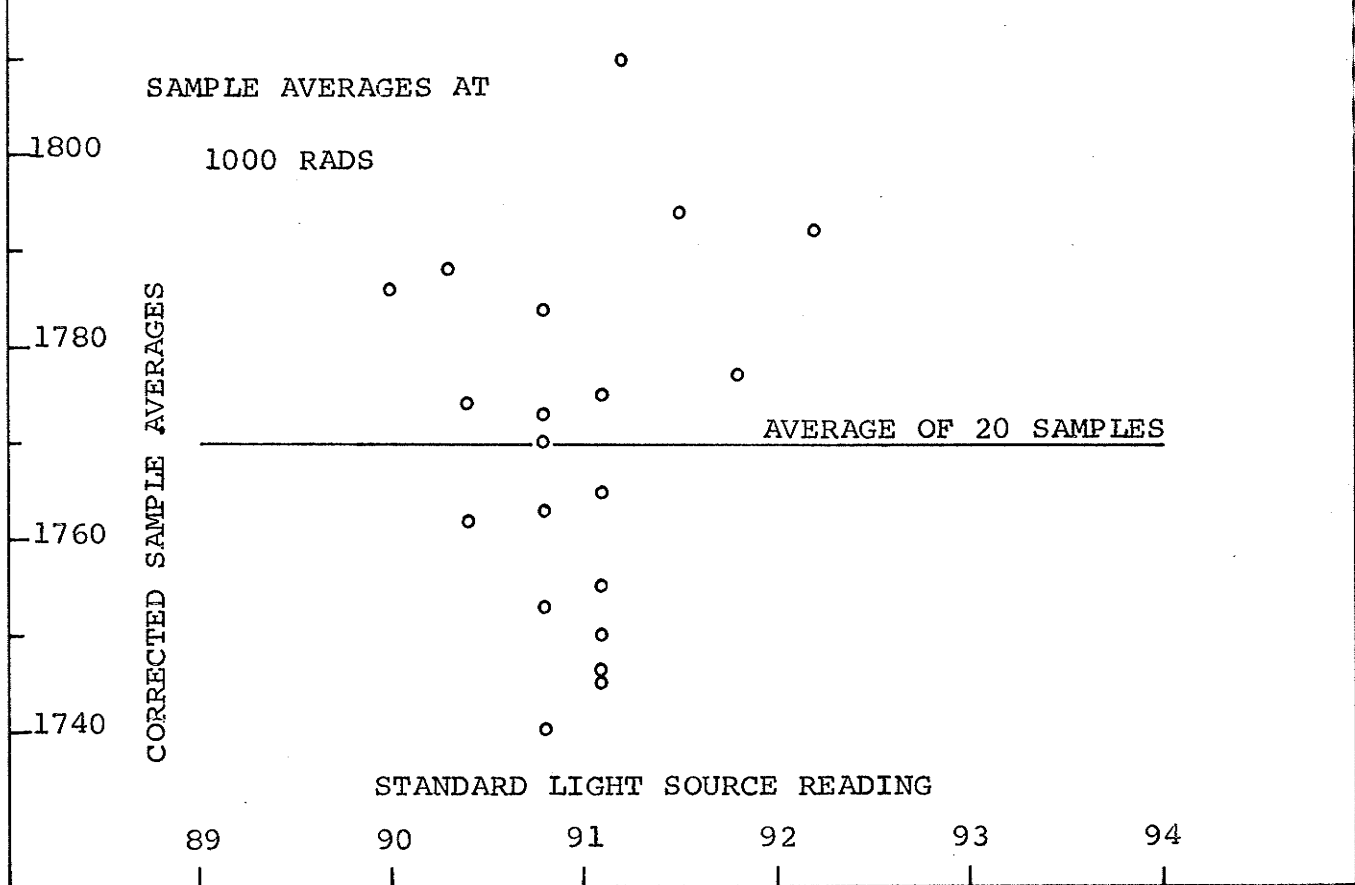


FIGURE 9-B.



The only difference between the two populations (100 rad and 1000 rad) was that the readings at 1000 rads were off scale. This meant that at the end of the integration the $\times 10$ scale switch was depressed. The voltmeter would then return rapidly to the proper reading but would overshoot in the direction toward zero. It would then take 60 - 90 seconds for it to climb slowly to the final reading. This allowed about a 2 minute cooling time between readings and is very likely the reason for the reduced drift. (In later experiments the drift at about 100 rads was reduced by allowing a 2 minute cooling time between readings.)

Karzmark⁴⁰ reported that light standards using a long lived radioactive source to excite a luminescent phosphor have a fluorescent intensity which depends markedly on temperature. The standard light source used above (C^{14} excites a luminescent phosphor) was heated above a water bath to temperatures as high as $80^{\circ}C$. and then immediately placed in the readout instrument. There was no change in the amount of light given off.

Heat, however, was the cause of the drift, because heating about 100 planchets (allowing no cooling time) caused the temperature in the photomultiplier housing to rise to about $38^{\circ}C$., and caused a 5 or 6% decrease in sensitivity to the C^{14} source. The temperature returned to $25^{\circ}C$. in about 2 hours, and the instrument recovered its original sensitivity during

this time.

The EMI 9536 S phototube in the Con-Rad readout instrument is of the venetian blind type. The photocathode is 4.3 cm. in diameter and is mounted on glass. At 100 rads, the anode current was less than $1\mu\text{A}$. and at 1000 rads it was 4 - 5 μA . peak. The photocathode current must be much smaller than that. A study of several papers^{12,40,41,42} on photo-multiplier fatigue has shown that saturation or photocathode fatigue are probably not responsible for the sensitivity drift. One possible cause is a reduced secondary emission factor due to increased temperature of the dynodes.⁴¹ One puzzling thing is that the change in sensitivity must be larger for the thermoluminescent light than it is for the standard light source light. If this is a wavelength dependence, then the photocathode must be responsible for the change in sensitivity.

Whatever the cause of the drift, it does not show up until about 10 readings have been taken, and then it can be nearly eliminated by allowing a 2 minute cooling time between readings. Even if the drift is ignored, the errors introduced into the dosimetry are not large.

C. ANNEALING PROCEDURE

Shortly after work began on the TLD system, some of the previously used powder was irradiated for a second time and when the energy was read out the response to 100 rads was found

to have doubled. Con-Rad had suggested annealing the powder for one hour at 400°C. (to release any trapped electrons from a previous irradiation) prior to re-use. After this was done the response to 100 rads was still 50% higher than what it had been originally.

This increased response was observed by Cameron and others and attributed to a low temperature peak in the glow curve produced by the previous irradiation. Cameron found that the new trapping centers, responsible for the low temperature peak, could be destroyed by annealing the powder for 24 hours at 80°C.^{10,11}

The used powder was annealed at 80°C. for 24 hours and the response dropped to its original value. It has since been found that the annealing temperature is quite critical. For example, 24 hour annealing at 83°C. did not quite return the response of the irradiated powder to normal. A temperature of 78° - 80° C. was found most efficient.

The standard annealing procedure recommended for re-use of the phosphor is therefore 400°C. for one hour followed by 78° - 80° C. for 24 hours. (It is desirable to remove the low temperature peak because the traps responsible for the peak are shallow and fading of the stored energy at room temperature would result.)

Calibration curves for unannealed powder are not constant multiples of curves for properly annealed powder. The

ratio of unannealed response to annealed response was 2 at 100 rads, 1.8 at 400 rads, and 1.7 at 700 rads. The curves slowly converge.

The annealing may also destroy some of the trapping centers in the original crystals. Powder that had been annealed and re-used about 10 times, and had received an accumulated dose of a few thousand rads showed a response 20% below the original response. (This fatigue was only measured at 20 to 140 rads.)

This fatigue may not be due to repeated annealing, but may be due to the accumulated dose. Capsules of powder that were given single doses of 10^4 to 10^5 rads (in obtaining Fig. 3) were kept separate from the rest. This powder was annealed and given doses of 60, 100, and 140 rads. The response was 56%, 53%, and 50% respectively of the original response. This decreased response is certainly a result of radiation damage, and not a result of prolonged annealing.

D. GLOW CURVES

In the last section it was stated that glow curves obtained with used powder exhibited a low temperature peak, and that this peak was responsible for increased fading of the total stored energy. It is suggested here that the readout cycle could be responsible for the low temperature peak. As the powder is heated to over 300°C ., vacancies would be created in the

crystal. Then when the heater shuts off after 10 seconds, the powder cools rapidly (to nearly room temperature in 15 - 20 seconds) freezing in the vacancies.

To investigate this a batch of LiF was properly annealed. Half the batch was heated to 400°C. and then dumped into a sieve to cool rapidly. Both halves of the batch were then irradiated to about 250 rads, and glow curves obtained for each.

Glow curves are normally obtained by monitoring the output of the phototube as a function of time (or temperature.) Since no device was available to monitor the P.M. tube output (less than 1 μ A.) a new method was devised. About 100 capsules of powder were dosed to 250 rads. The powder was all tipped into a test tube and placed in an oven. The oven temperature was then increased uniformly at the rate of 1 degree per minute. Every 5 minutes (or 5 degrees) about 180 mg. of powder was lifted out of the test tube and dispensed into planchets. Then the energy remaining in the powder was determined and the remaining response was plotted against oven temperature. (Fig. 10.) (The error bars give the maximum and minimum of 3 readings while the circle gives the average of 3 readings.) The slope of this curve is the energy released per unit temperature interval and is therefore proportional to the height of a glow curve. This slope was plotted vs. temperature to give the glow curves of

FIGURE 10.

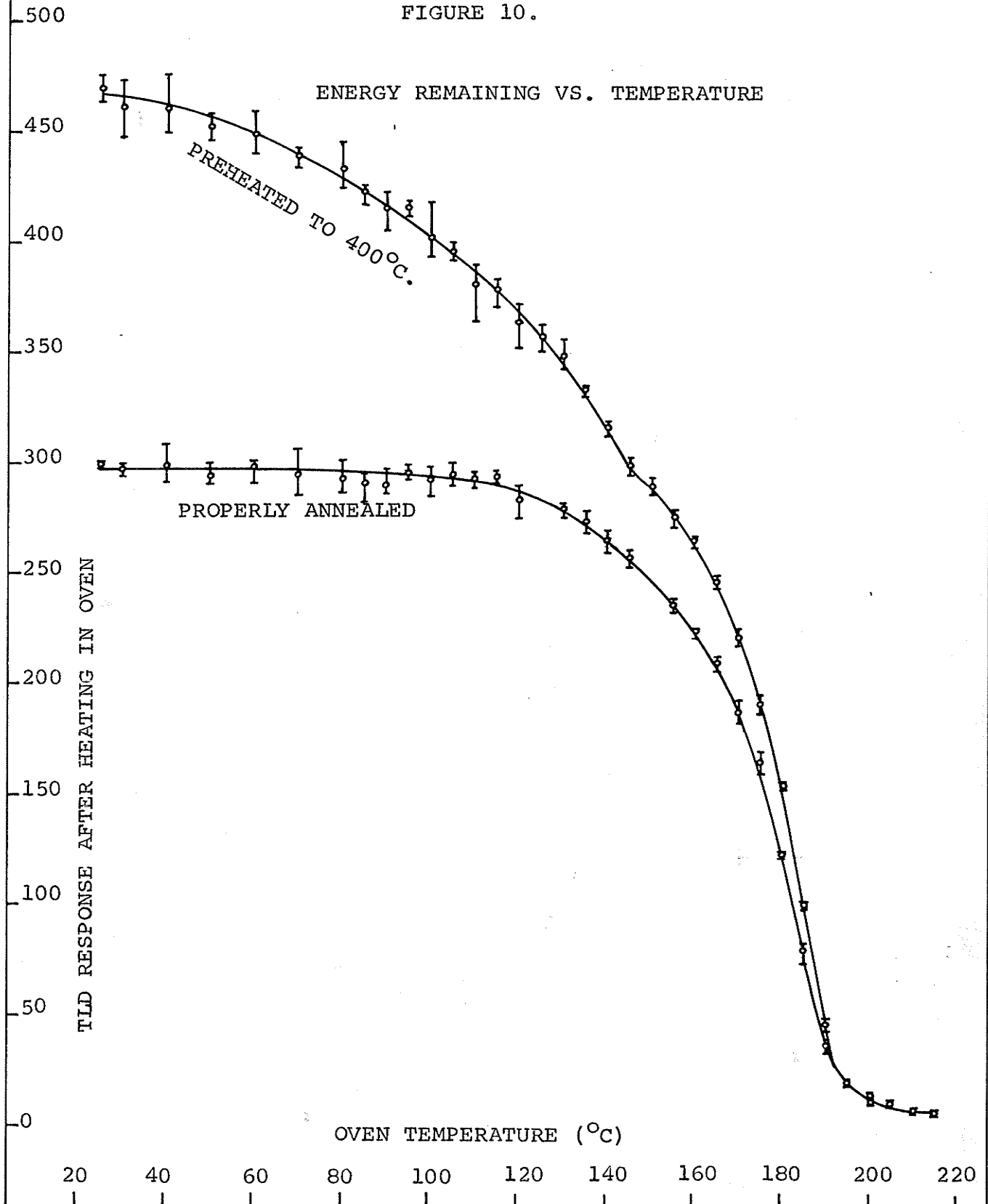


Fig. 11. Both curves have peaks at 185°C., 140°C., and at 70°C. - 80°C., although the low temperature peaks are much more pronounced with powder that had been heated and rapidly cooled.

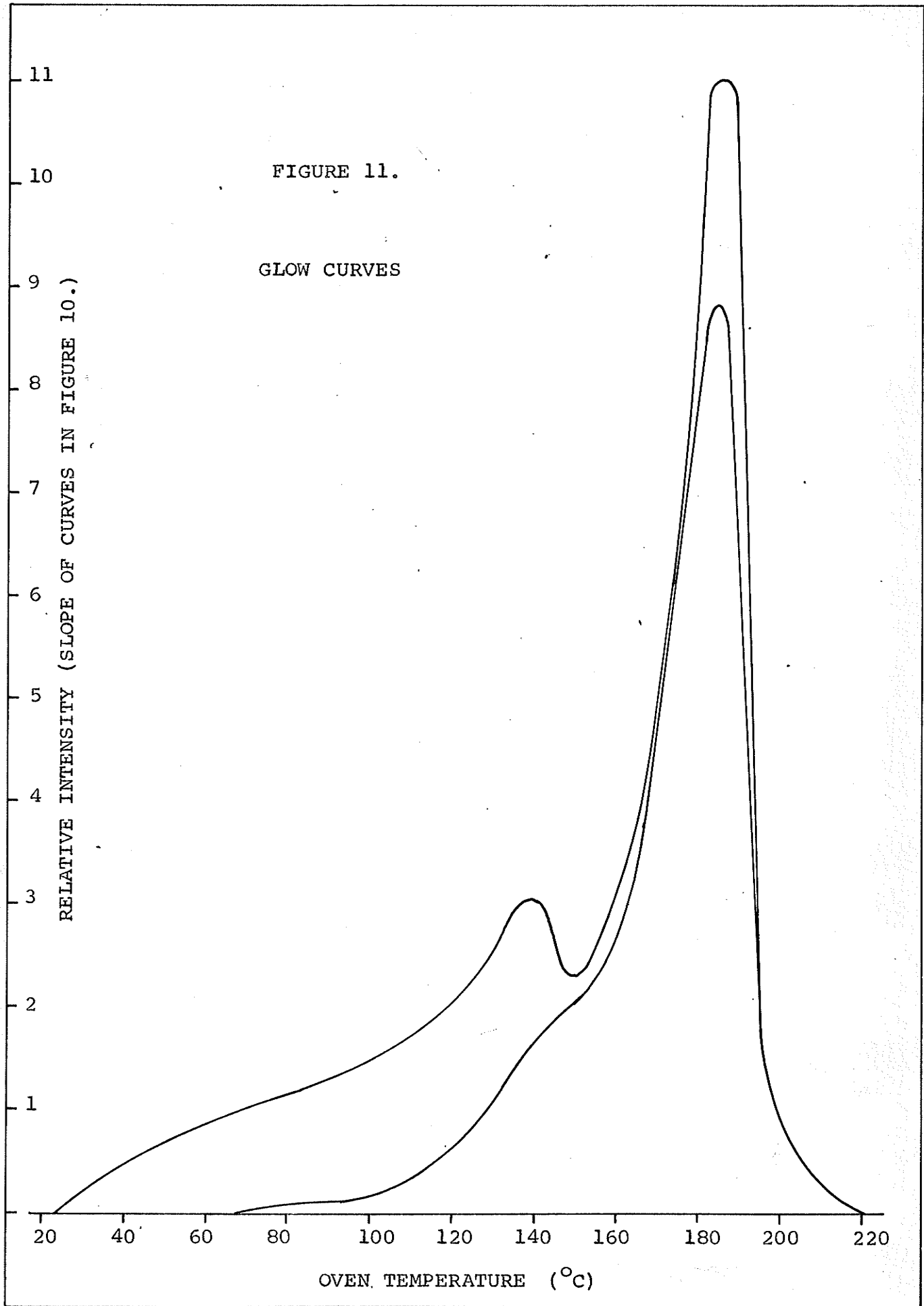
Powder that was run through a readout cycle before irradiation showed a 60% increase in response due to these low temperature peaks. Powder that was irradiated to 100 rads, and then read out showed a 100% increase in response when irradiated again without further annealing. Therefore, 60% of the increase could be attributed to the readout cycle and 40% to the previous irradiation. This 40% also appears to be due to an increase in the number of shallow traps, as evidenced by a further increase in the low temperature peaks with used powder. It should be noted that the glow curve for used powder was obtained in a somewhat different manner to those in Fig. 11, (a plot analogous to Fig. 10 was obtained by heating 5 capsules of irradiated powder directly to the desired temperature, and then measuring the energy remaining in the powder. There was, therefore, no uniform heating rate) and because of this the evidence is not conclusive.

E. TRAP DEPTH

From equations (13.) and (16.) of chapter three, the intensity of the thermoluminescence may be expressed as

FIGURE 11.

GLOW CURVES



$$I = n / \tau = n S e^{-E/kT} \dots \dots \dots (23.)$$

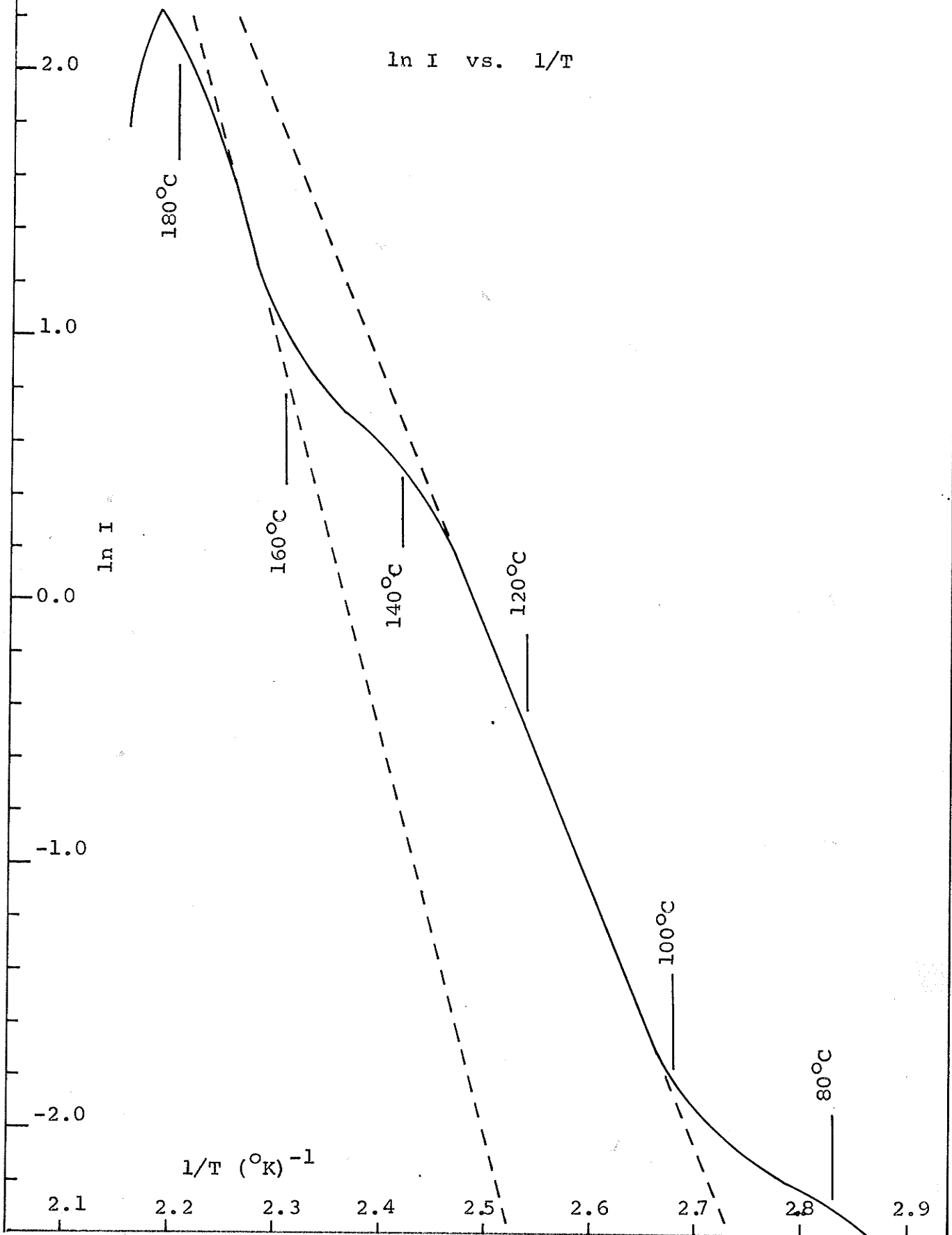
The number of filled traps, n , of course is not a constant, but is continually changing along the glow curve according to (17.) Assuming that n is constant near the beginning of a glow curve, a plot of $\ln I$ vs. $1/T$ should yield a linear region of slope E/k . Morehead and Daniels⁶ found a trap depth $E = 1.4$ ev. from such a plot.

In Fig. 12 $\ln I$ was plotted vs. $1/T$, the data being obtained from the glow curve for properly annealed powder in Fig. 11. At $1/T = 2.92$ the curve approaches $-\infty$; it is linear from 2.46 to 2.67, and roughly linear around the inflection point at 2.27. The two linear regions correspond to temperatures near the beginning of the second and third glow peaks of Fig. 11. Setting the slopes of these two regions equal to E/k gave trap depths of 0.84 ev. and 1.25 ev. respectively. The value of 1.25 ev. may easily be too low since the curve in Fig. 12 would not reverse curvature at $1/T = 2.27$ if it were not for the presence of the low temperature peak in the original glow curve. Even if the low temperature peaks could be completely eliminated, there would be difficulty in choosing the correct slope. This is because at the beginning of a glow curve (temperature T_i) I must be zero, and hence $\ln I$ must approach $-\infty$ as $1/T$ approaches $1/T_i$.

Another method, based on equation (20.), page 31, was

FIGURE 12.

$\ln I$ vs. $1/T$



also used to determine the trap depth. This method uses the fact that the position of a glow peak depends on the heating rate used in obtaining the glow curve. Karzmark et al.¹⁴ obtained glow curves by monitoring the output of a photomultiplier tube while the powder was heated at a uniform rate. In order to obtain a measurable intensity large heating rates had to be used. They found the main glow peak at 220°C. for a heating rate of 260 degrees/min. It was assumed that the traps in Karzmark's LiF (TLD-100) were of the same nature as the traps in the powder used in Fig. 11 (Con-Rad type-N), and the values $B_1 = 1$ degree/min., $B_2 = 260$ degrees/min., $T_1^* = 185^\circ\text{C.} = 458^\circ\text{K}$, and $T_2^* = 220^\circ\text{C.} = 493^\circ\text{K}$ were substituted into equation (20.) This gave a trap depth $E = 3.0$ ev., considerably larger than the values found previously. As a further check, a glow curve was run with properly annealed powder using a heating rate $B_1 = 1.4$ degrees/min. The main glow peak was found between 188°C. and 190°C. Using $T_1^* = 188^\circ\text{C.}$ in equation (20.) along with Karzmark's data gave $E = 3.1$ ev. and using $T_1^* = 190^\circ\text{C.}$ gave $E = 3.5$ ev.

Both these methods were based on the Randall and Wilkins model of thermoluminescence. The second method involved no assumptions except that the two types of powder involved had the same kind of traps. This is probably a valid assumption. The first method assumed that n was constant at the beginning of a glow curve but in this region the curve had to approach $-\infty$. The choice of slope for one glow peak was made difficult by the

presence of the next lower peak. It is therefore felt that the second method was more accurate, although it is recognized that both methods were based on a simplified model which may not accurately describe the mechanism of thermoluminescence in LiF.

F. FADING OF STORED ENERGY

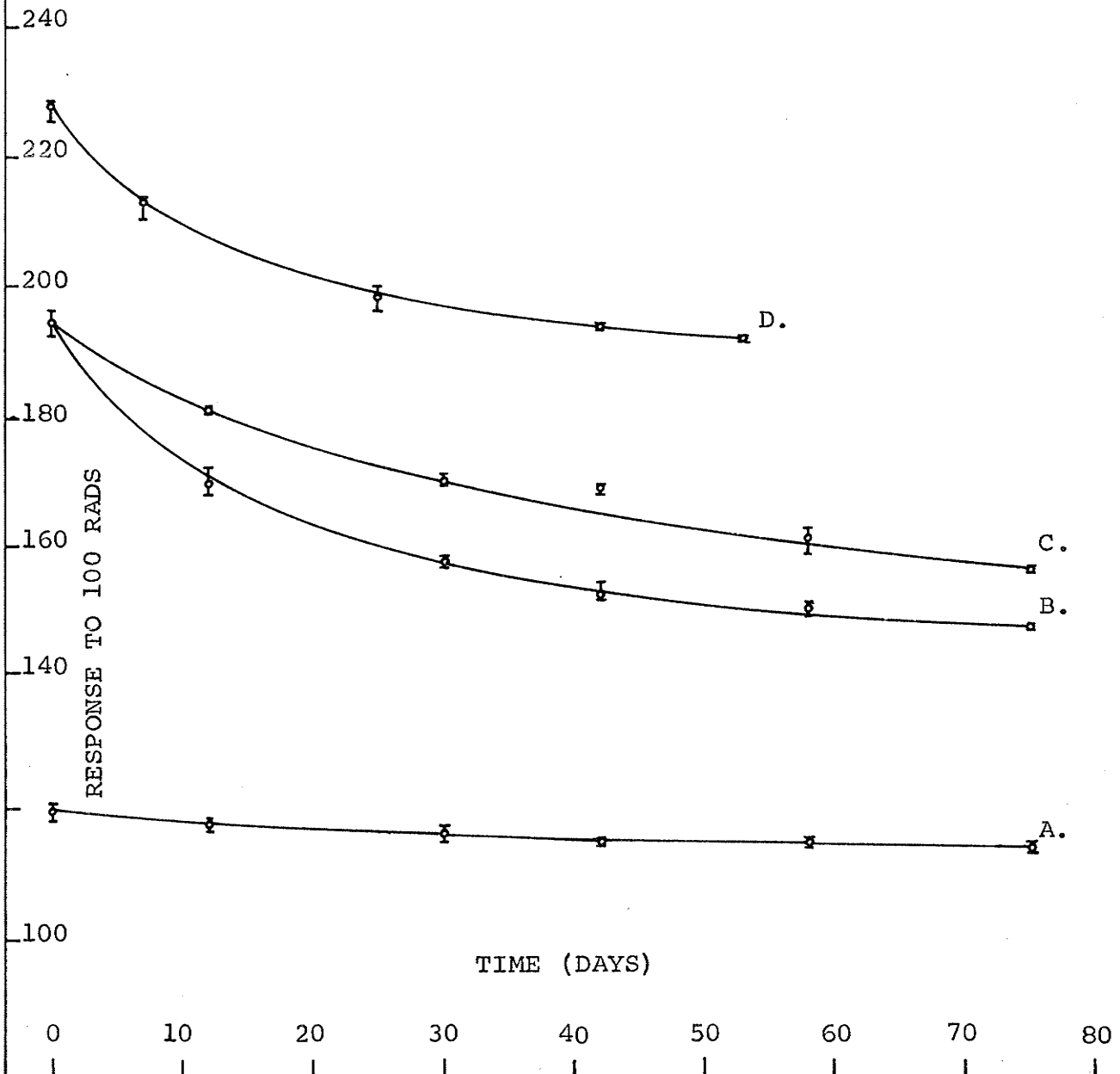
Several experiments were done to determine the extent of the fading with powder treated in various ways. The experiments were started with new powder which was supposed to have been annealed by the manufacturer before shipment.

The results for type-N powder are shown in Fig. 13. Curve A was obtained by irradiating the new powder to 100 rads on day zero, and then reading out the stored energy immediately after, as well as every 12 - 15 days thereafter. Curve B was obtained by running some of the new powder through a readout cycle to create shallow traps. It was then irradiated to 100 rads and read out immediately after as well as every 12 - 15 days thereafter. Curve C was obtained by running some of the new powder through a readout cycle on day zero. Then every 12 - 15 days, three capsules were irradiated to 100 rads and read out immediately after. Curve D was obtained by irradiating new powder to 100 rads, and then running it through a readout cycle. This used powder was then given another 100 rads and the response was measured immediately as well as every 12 - 15 days thereafter.

New powder (curve A) showed a 5% fading after 75 days,

FIGURE 13.

FADING OF TYPE-N LiF



most of the fading occurring during the first 30 days. Some fading was expected because as Fig. 11 showed, the shallow traps are not completely destroyed by the standard annealing procedure. Cameron et al¹⁰ reported a fading of less than 5% in one year. It is quite possible that the powder used here was annealed for less than 24 hours, or at a temperature slightly different from 80°C. This would account for the increased fading. To show how critical the annealing temperature is, some new powder was annealed at 400°C. for 1 hour (this would create vacancies in the crystals) and then for 24 hours at 82°C. (instead of 78° - 80°). The response of this powder was up to 129, an increase of 7% over the new powder, and the fading was 6% over the first month compared to 3% for new powder.

Powder which had been run through a readout cycle just prior to irradiation stored 61% more energy than the new powder, but lost 24% of the total stored energy over the first 75 days (curve B.) This was expected because of the increased number of shallow traps. The 24% fading could be accomplished by the escape of 24% of the trapped electrons. There is also the possibility that the shallow traps are slowly destroyed at room temperature. (Since a temperature of 80°C. destroys nearly all the shallow traps in one day, a temperature of 22°C. may destroy an appreciable number in 75 days.) To investigate this, the fading due to electron escape was eliminated by irradiating just

before the readout (curve C.) The time axis in Fig. 13 then represents the time that the powder sat, unirradiated, at room temperature, after creation of the shallow traps. Curve C shows that 19% of the total number of traps were destroyed at room temperature in 75 days. These results indicate that the standard annealing procedure is necessary, even if the energy is to be read out immediately after irradiation, because a calibration curve obtained with used powder one week could be out by 8% two weeks later due to destruction of shallow traps.

Curve D was obtained with used powder, but unfortunately the powder was used a few days before the second irradiation. The second irradiation was done on day zero. During those few days some of the shallow traps would have been destroyed, and the powder was able to store only 90% more energy than the new powder (instead of 100% more as was found previously.) Even if the curve D is displaced to the right by 5 or 6 days, and the initial response assumed to be about 240, the fading is still no more severe than for powder B. If anything, the fading is less severe, and this would indicate that the traps created by the previous irradiation were deeper than the ones created by the heating and rapid cooling. This contradicts the results stated in section D but because of factors unknown at the beginning of each experiment, neither investigation with used powder was conclusive.

Similar fading curves were obtained with type-7 powder.

FIGURE 14.

FADING OF TYPE-7 LiF

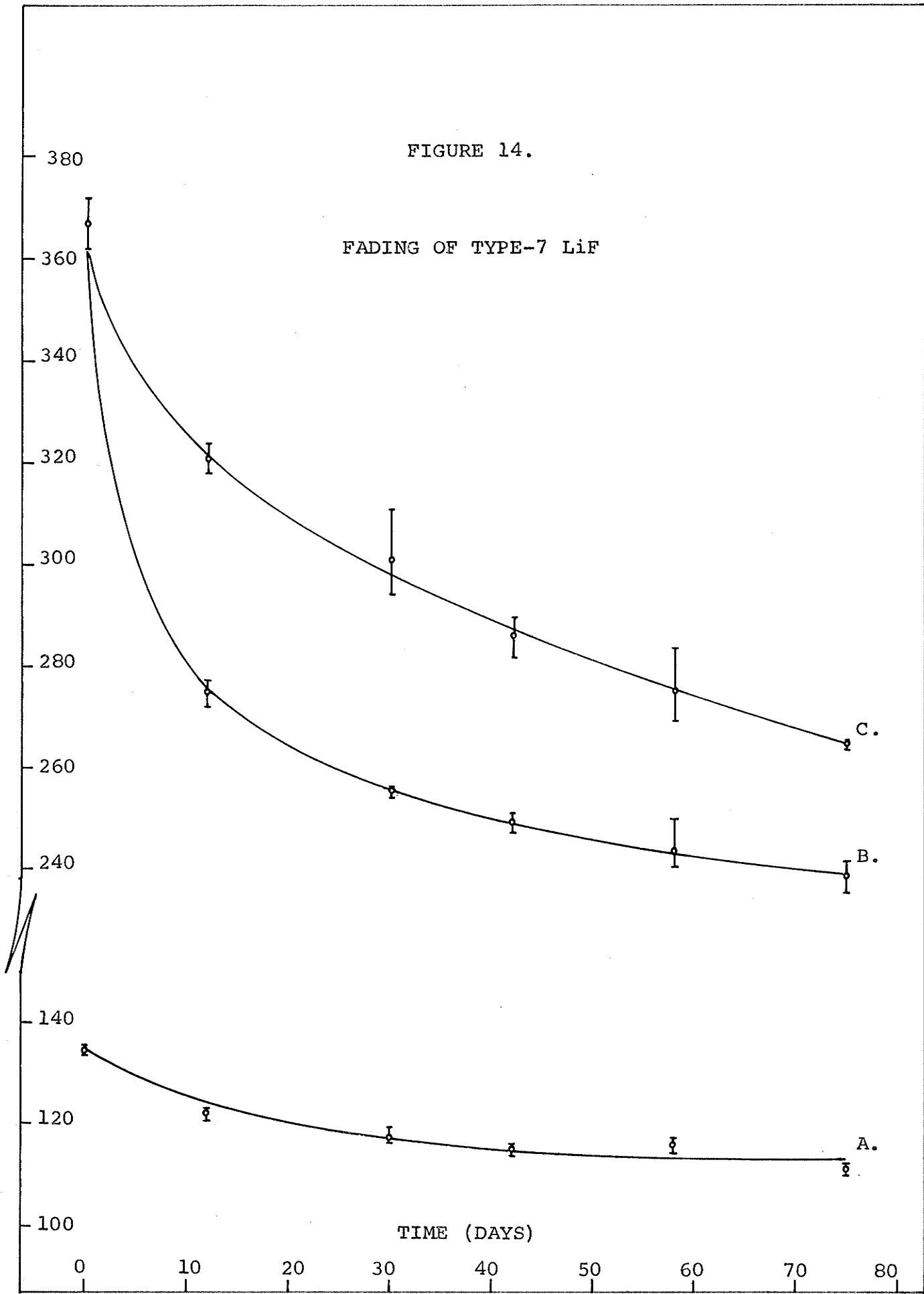


(Fig. 14.) (It was stated in the Con-Rad instruction manual that annealing was more important for type-7 powder.) The response to 100 rads at day zero was 134, for new powder, and the fading amounted to 16% over 75 days so that the fading curve approached the curve for type-N. The increased fading was probably because of improper annealing by the manufacturer. The type-7 powder was much more susceptible to the heating cycle, increasing in response by nearly 200%. The fading of the heated powder was also much more severe than it was for type-N. (Curves A, B, and C of Fig. 14 were obtained in the same way as curves A, B, and C of Fig. 13.)

G. RESPONSE OF OTHER LiF

Because of the high cost of the "specially activated" lithium fluoride supplied by Con-Rad, lithium fluoride from two other sources was investigated for thermoluminescent response.

Some large crystals of LiF were obtained from the solid state section of the University of Manitoba Physics Department. The past history of these crystals was unknown. There was a remote possibility that an attempt had been made to instill F centers in some of the crystals by diffusion of excess Li into the crystal. These large crystals were ground to the same size as the Con-Rad crystals (100 - 200 mesh sieve), and were then run through a readout cycle. No response was found. They were then properly annealed and irradiated with Co^{60} gamma

rays. The response was found to be only 15% of the Con-Rad LiF response at 100 rads, and 10% at 2000 rads. This would still be sufficient for a useful dosimeter. (The final reading could be increased by increasing the voltage on the dynodes of the photomultiplier tube.)

A very finely ground LiF from the J. T. Baker Chemical Co. was irradiated. Fifty mg. of this powder gave a response of $\frac{1}{2}\%$ of that for the Con-Rad LiF. Because of the very small crystal size this powder could not be dispensed, nor could it be leveled in the planchet.

It appears that the activation not only results in an increased response to low doses, but also in an increased rise in the response/rad vs. rads curve. This suggests that less activation would give more linear dose response curves, and may account for the fact that curves obtained by Cameron with TLD-100 were more linear.

CHAPTER VI

CONCLUSIONS

Thermoluminescence in LiF has shown itself to be a useful tool in clinical radiation dosimetry. Because of its small size and simplicity of use, the dosimeter has in vivo applications such as depth dose measurement, dose distribution in whole body irradiation, intracavitary dosimetry, and dose confirmation for radioactive implants. Other uses are beam calibration for both electromagnetic and corpuscular radiation, and even half-value layer determinations.

With some care in dispensing the powder, in leveling the powder in the planchet, and in supplying the right amount of heat to the planchet, the precision of any measurement can be within 2% of the correct value. If several measurements are to be taken a two minute cooling time between samples is recommended.

The unwanted annealing at room temperature, and the fading of the stored energy at room temperature should not result in errors of more than two percent over a few months provided the powder is properly annealed after each use. For most clinical measurements of less than a few thousand rads there is

no need to separate the powder according to dose received. The powder need only be classified as "used" or "annealed".

The accuracy with which a measured response can be converted to an absorbed dose depends on the care taken in calibrating the powder. Figures 3 - 8 present calibration curves for Co^{60} gamma rays, for x-rays generated at 100 kv. and 250 kv. and for electrons at 25 Mev. and 35 Mev. Unfortunately, since these curves were obtained the powder has been used and annealed several times, and, because of a change in sensitivity, the absolute magnitude of the response curves no longer applies. However, the curves of Figures 5 - 8 were all obtained with the same batch of powder and may be used as a basis for all future calibrations. Assuming that the decrease in sensitivity (fatigue) is independent of the dose to be received, and independent of the radiation which delivers the dose, then, after annealing a batch of powder, only one calibration point (say 100 rads from Co^{60}) need be re-determined. The factor required to normalize the response per rad for this point to the Co^{60} curve in Fig. 7 may then be used to correct all the other curves for fatigue. Alternately, the instrument sensitivity may be adjusted to bring the response per rad to the value given in Fig. 7. (Cobalt radiation was chosen for the normalization because for a given geometry the dose rate has been accurately determined and need only be corrected for decay of the source.)

The normalization described above was based on two assumptions which may not be valid. It was shown in section C that the fatigue of heavily dosed powder was 3% greater at 140 rads than it was at 60 rads. This could become a serious problem when the total fatigue is greater than a few percent. Further investigation is necessary to determine the dose dependence at higher doses, and to determine the effects of fatigue with other radiations.

Some of the experiments performed and the conclusions drawn had little connection with clinical dosimetry. A simple model for the mechanism of energy storage in LiF was proposed to explain the dose dependence of the response curves. The model involves two processes within the crystal, the creation of new traps and the filling of existing traps with electrons. It was suggested that the traps might be negative ion vacancies which would become F centers after having trapped an electron released by the ionizing radiation. It was further suggested that the secondary electrons, released in the crystal by the gamma rays or x-rays, as well as the electrons from the betatron, might create vacancies by dislodging ions along a dislocation edge where the ionic binding is reduced. On this model the increase in response per rad with increasing dose would be expected if vacancies were created faster than they were filled

with electrons. The fact that secondary electrons of higher energy result in a more pronounced increase in response per rad would also be expected due to their increased ability to produce vacancies.

Experiments with LiF which was not specially activated showed less increase in response per rad with dose, as well as an overall reduction in response. The drop in the response per rad curve could be due to fewer ion vacancies and the flattening of the curve could be due to fewer dislocation edges.

A new method of obtaining glow curves, involving very low heating rates, was devised. Three peaks were found in all glow curves, the magnitude of the lower temperature peaks being greatly increased by heating the crystals and then cooling them rapidly. This was explained as a "freezing in" of vacancies created by the high temperature. These "vacancies" are apparently not the same as the "vacancies" referred to in the above model. (because they result in shallower traps.) The simple model may therefore have to be changed by replacing the word "vacancy" by "trapping center" where a trapping center is some combination of positive and negative ion vacancies, electrons and holes, which can trap an electron. Such aggregates are not uncommon in alkali halide crystals.

The main trap depth in LiF was determined by two different methods. The values obtained were 3.0 ev. and 1.25 ev., the first value probably being the more accurate one. Both

methods were based on a simple model involving a single trap depth. No attempt was made to further study the mechanism of the release of electrons from traps.

BIBLIOGRAPHY

1. F. W. Spiers, "Radiation Units and Theory of Ionization Dosimetry" in Radiation Dosimetry, G.J. Hine & G.L. Brownell, editors, (Academic Press Inc., New York, 1956)
2. John F. Fowler, *Phys. Med. & Biol.* 8, 1 (1963)
3. John F. Fowler, *Nucleonics* 21, 60 (October, 1963)
4. International Commission on Radiological Units and Measurements (ICRU), Report 10b, 1962, Physical Aspects of Irradiation, (NBS Handbook 85), section I F
5. F. Daniels, C. A. Boyd, and D. F. Saunders, *Science* 117, 343 (1953)
6. F. F. Morehead and F. Daniels, *J. Chem. Phys.* 27, 1318 (1957)
7. F. Daniels and W. P. Rieman, Chemical Procurement Agency, Wash., D.C., Final Report, Project number 4-12-80-001 (1954)
8. J. R. Cameron et al., *Science* 134, 333 (1961)
9. J. R. Cameron and G. Kenney, *Radiation Research* 19, 199 (1963)
10. J. R. Cameron, D. Zimmerman, and G. Kenney, *Radiation Research* 19, 199 (1963)
11. J. R. Cameron et al., *Health Physics* 10, 25 (1964)
12. G. Kenney, J. R. Cameron, and D. Zimmerman, *Rev. Sci. Instrum.* 34, 769 (1963)
13. R. C. McCall, L. E. Babcock, and R. C. Fix, *Radiation Research* 19, 200 (1963)
14. C. J. Karzmark, John White, and J. F. Fowler, *Phys. Med. & Biol.* 9, 273 (1964)
15. M. J. Marrone and F. H. Attix, *Health Physics* 10, 431 (1964)

16. Controls for Radiation Inc. (bulletin)
17. H. E. Johns and J. S. Laughlin, "Interaction of Radiation with Matter" in Radiation Dosimetry, G.J. Hine & G.L. Brownell, editors, (Academic Press Inc., New York, 1956)
18. A. H. Compton and S. K. Allison, X-Rays in Theory and Experiment, (Van Nostrand, New York, 1946)
19. W. Heitler, Quantum Theory of Radiation, third edition, (Oxford University Press, 1954)
20. International Commission on Radiological Units and Measurements (ICRU), Report 10b, 1962, Physical Aspects of Irradiation, (NBS Handbook 85), section I A 3
21. International Commission on Radiological Units and Measurements (ICRU), Report 10d, 1962, Clinical Dosimetry, (NBS Handbook 87), section IV F
22. W. H. Bragg, Studies in Radioactivity, (Macmillan, New York, 1912)
23. L. H. Gray, Proc. Roy. Soc. A 156, 578 (1936)
24. L. H. Gray, Brit. J. Radiol. 10, 600, 721 (1937)
25. D. V. Cormack and H. E. Johns, Rad. Research, 1, 133 (1954)
26. G. N. Whyte, Nucleonics 12, 19, (February, 1954)
27. National Committee on Radiation Protection and Measurements (NCRP), Report No. 27, 1961, Stopping Powers For Use With Cavity Chambers, (NBS Handbook 79)
28. E. Fermi, Phys. Rev. 57, 445 (1940)
29. O. Halpern and H. Hall, Phys. Rev. 57, 459 (1940)
30. O. Halpern and H. Hall, Phys. Rev. 73, 477 (1948)
31. R. M. Sternheimer, Phys. Rev. 88, 851 (1952)
32. R. M. Sternheimer, Phys. Rev. 103, 511 (1956)

33. G. V. Taplin, "Chemical and Colorimetric Indicators", in Radiation Dosimetry, G.J. Hine & G.L. Brownell, editors, (Academic Press Inc., New York, 1956)
34. D. Curie, Luminescence in Crystals, translated by G.F.J. Garlick, (Methuen & Co., Ltd., London, 1963)
35. J. T. Randall and M. H. F. Wilkins, Proc. Roy. Soc. A 184, 366 (1945)
36. H. E. Johns, The Physics of Radiology (Thomas, Springfield, Illinois, 1961) p. 281
37. B. Petree and J. C. Humphreys, Radiology 84, 128 (1965)
38. J. W. Scrimger and D. V. Cormack, Brit. J. Radiol. 36, 514 (1963)
39. M. J. Moroney, Facts From Figures, (Penguin Books Inc., Baltimore, 1956)
40. C. J. Karzmark, Health Physics 11, 54 (1965)
41. J. P. Keene, Rev. Sci. Instrum. 34, 1220 (1963)
42. Kiyoshi Miyake, Rev. Sci. Instrum. 32, 929 (1961)
43. R. M. Sternheimer, (private communication, 1965)

APPENDIX A

CALCULATION OF ABSORPTION COEFFICIENTS

In calculating the ratio $(u/\rho)_{\text{LiF}} / (u/\rho)_{\text{H}_2\text{O}}$ for cobalt radiation, only Compton interactions were considered. The scattered radiation in the beam (see footnote page 44) would introduce some photoelectric absorption but the net amount was considered negligible in both LiF and water. Pair production contributes a negligible amount in both materials at 1.33 Mev.

The mass absorption coefficient is a product of the electronic absorption coefficient and the number of electrons per gram of material.

$$u/\rho = (NZ/M) (\rho_e u) \dots \dots \dots (A-1.)$$

For the Compton effect, the electrons are considered as free, and therefore $\rho_e u = \rho_e \sigma$ is independent of the absorbing material. The ratio of the absorption coefficients is therefore just the ratio of the numbers of electrons per gram.

For compounds Z is the effective atomic number, and is 12 for LiF and 10 for H₂O. The molecular weight, M, is 25.94 for LiF and 18 for H₂O. Thus

$$\frac{(u/\rho)_{\text{LiF}}}{(u/\rho)_{\text{H}_2\text{O}}} = \frac{(ZN/M)_{\text{LiF}}}{(ZN/M)_{\text{H}_2\text{O}}} = 0.833 \dots \dots \dots (A-2.)$$

APPENDIX B

CALCULATION OF STOPPING POWERS

Equation (11.), page 26 gives the stopping power for electrons per electron of the absorbing material. If this is multiplied by n , the number of electrons per cm.^3 , and divided by ρ , the density of the medium, one obtains the mass stopping power of the medium, m^S , which may be expressed in $\text{Mev. per gm./cm.}^2$. The resulting expression, which may be shown to be identical with the expression for m^S as stated in Handbook 79²⁷, may be re-written as

$$m^S = \frac{A}{\beta^2} \left[B + 2 \ln(P/m_0 c) + \ln T - \ln 2 + (1 - \beta^2) - (2 \sqrt{1 - \beta^2} - 1 + \beta^2) \ln 2 + \frac{1}{8} (1 - \sqrt{1 - \beta^2})^2 - \delta \right] \dots (B-1.)$$

where $A = 2 \pi n e^4 / m_0 c^2 \rho \dots \dots \dots (B-2.)$

and $B = \ln [m_0 c^2 (10^6 \text{ ev.}) / I^2] \dots \dots \dots (B-3.)$

and where T is the incident electron energy in Mev. ,
 $P = mv = m \beta c$ is the electron momentum, and δ is the density correction. The equation was written in this form for easy comparison with Sternheimer's papers of 1952 and 1956.^{31,32} The density correction was calculated by the method of Sternheimer.³¹

The values of A for LiF and H_2O are listed in table B-1 expressed in $\text{Mev. per gm./cm.}^2$. The value of ρ for LiF was taken as 2.601 gm./cm.^3 from the Handbook of Chemistry and Physics,

forty-fourth edition, Chemical Rubber Publishing Co. The value given in the American Institute of Physics Handbook is in error.

(Dr. H. P. R. Frederikse - private communication)

The values of B are also listed in table B-I. The mean ionization potential, I, for LiF and for H₂O was calculated from the mean ionization potentials of the constituent atoms using

$$\ln I = \sum_i (Z_i / Z) \ln I_i \dots \dots \dots (B-4.)$$

For both lithium and fluorine the relation $I = 13Z$ was used as suggested by Sternheimer.⁴³ This gives $I = 39$ ev. for lithium in good agreement with Bakker and Segre's value of 38 ev. quoted in Handbook 79.²⁷ Although no data was available for fluorine, $I = 13Z$ was a good approximation for the elements with Z near 9, and hence was assumed to hold for fluorine. For hydrogen and oxygen the values of 17.6 ev. and 98.5 ev., respectively, were taken from table 3 of Handbook 79.²⁷ The values of I are listed in table B-1 in rydberg units (1 ry. = 13.6 ev.)

The density correction, δ , as derived by Sternheimer is given by

$$\delta = \sum_i f_i \ln \left[\frac{(\bar{\nu}_i^2 + \mathfrak{L}^2)}{\bar{\nu}_i^2} \right] - \mathfrak{L}^2 (1 - \beta^2) \dots \dots (B-5.)$$

where f_i is the oscillator strength of the i^{th} transition whose frequency is $\bar{\nu}_i$, and \mathfrak{L} is a frequency given by

$$\frac{1}{\beta^2} - 1 = \sum_i \frac{f_i}{\bar{\nu}_i^2 + \mathfrak{L}^2} \dots \dots \dots (B-6.)$$

Here, $\bar{\nu}_i$ is to be expressed in terms of the plasma frequency of the medium which is given by

$$\nu_p = \left[\frac{n e^2}{\pi m_0} \right]^{1/2} \dots \dots \dots (B-7.)$$

The method from here on is identical with Sternheimer's. (1952.) As a first approximation the frequencies were found from the ionization potentials, $h\nu_i$, of the K, L, M, etc. shells. These appear in table B-I expressed in rydberg units, and were taken from the tables of critical x-ray absorption energies on page 2776 of the Handbook of Chemistry and Physics, and page 7-136 of the American Institute of Physics Handbook, wherever possible. For LiF, $h\nu_1$ pertains to the K level of Li, $h\nu_2$ to the L level; $h\nu_3$ to the K level of F, $h\nu_4$ to the L_I level, and $h\nu_5$ to the $L_{II,III}$ level. For H₂O, $h\nu_1$ pertains to the K level of O, $h\nu_2$ to the L_I level, $h\nu_3$ to the $L_{II,III}$ level; and $h\nu_4$ to the K level of H.

The values of $h\nu_2$ of LiF and $h\nu_4$ of H₂O are first ionization potentials and were taken from page 7-14 of the American Institute of Physics Handbook.

The values of $h\nu_4$ of LiF and $h\nu_2$ of H₂O were not listed and were determined by extrapolation from L_I levels of elements of higher atomic number.

TABLE B-I

	<u>LiF</u>	<u>H₂O</u>		<u>LiF</u>	<u>H₂O</u>
A	.0711	.0853	$h\nu_5$	0.9	-----
B	17.98	18.47	$h\nu'_1$	6.17	115.0
I	6.54	5.13	$h\nu'_2$	0.61	5.9
f_1	2/12	2/10	$h\nu'_3$	159.0	2.05
f_2	1/12	2/10	$h\nu'_4$	7.8	1.29
f_3	2/12	4/10	$h\nu'_5$	2.8	-----
f_4	2/12	2/10	$h\nu_p$	2.33	1.58
f_5	5/12	-----	$\bar{\nu}_1$	2.65	72.8
$h\nu_1$	4.0	39.3	$\bar{\nu}_2$	0.26	3.7
$h\nu_2$	0.4	2.0	$\bar{\nu}_3$	68.2	1.3
$h\nu_3$	51.0	0.7	$\bar{\nu}_4$	3.35	0.82
$h\nu_4$	2.5	1.0	$\bar{\nu}_5$	1.20	-----

The $h\nu_i$ thus determined were then corrected by the factor $I/h\nu_m$ where I is the mean ionization potential of one of the constituent atoms, and $h\nu_m$ is the geometric mean of the $h\nu_i$ for that constituent atom. Thus, a different correction factor was obtained for each constituent atom, and the corrected energies ($h\nu'_i$) are listed in table B-I. For Li, the geometric mean, $h\nu_m$, of $h\nu_1$ and $h\nu_2$ is 1.87 ry. and $I = 39$ ev. = 2.87 ry. Thus $I/h\nu_m = 1.53$. For F, $h\nu_m = 2.77$ ry. and $I = 8.6$ ry. and therefore $I/h\nu_m = 3.10$. For O, $h\nu_m = 2.49$ ry. and $I = 7.3$ ry. giving $I/h\nu_m = 2.93$. For H, $h\nu_m = 1$ ry. and $I = 1.29$ ry.

giving $I/h\nu_m = 1.29$.

Finally, the $\bar{\nu}_i$ were determined from the $h\nu'_i$ by dividing by $h\nu_p$, where ν_p is given by equation (B-7.) and is listed in table B-I in rydbergs.

The values of \mathcal{A} at various energies were determined graphically by plotting equation (B-6.)

The density correction, δ , is plotted as a function of $\log_{10} (P/m_0c)$ in Fig. B-1 for easy comparison with Fig. 1 of Sternheimer's paper of 1952.

From the data of table B-I and from Fig. B-1 the mass stopping powers for LiF and H₂O were calculated using equation (B-1.) The results are shown in Fig. B-2 as a function of electron energy. (The dashed curves are not corrected for the density effect.)

The ratio of the stopping powers for various energies are given in table B-II.

TABLE B-II

<u>Electron Energy (Mev.)</u>	<u>($m S$)_{LiF} / ($m S$)_{H₂O}</u>
0.2	0.806
0.5	0.806
1.0	0.808
2.0	0.809
5.0	0.809
10.0	0.809
20.0	0.808
50.0	0.808

FIGURE B-1.

DENSITY CORRECTION

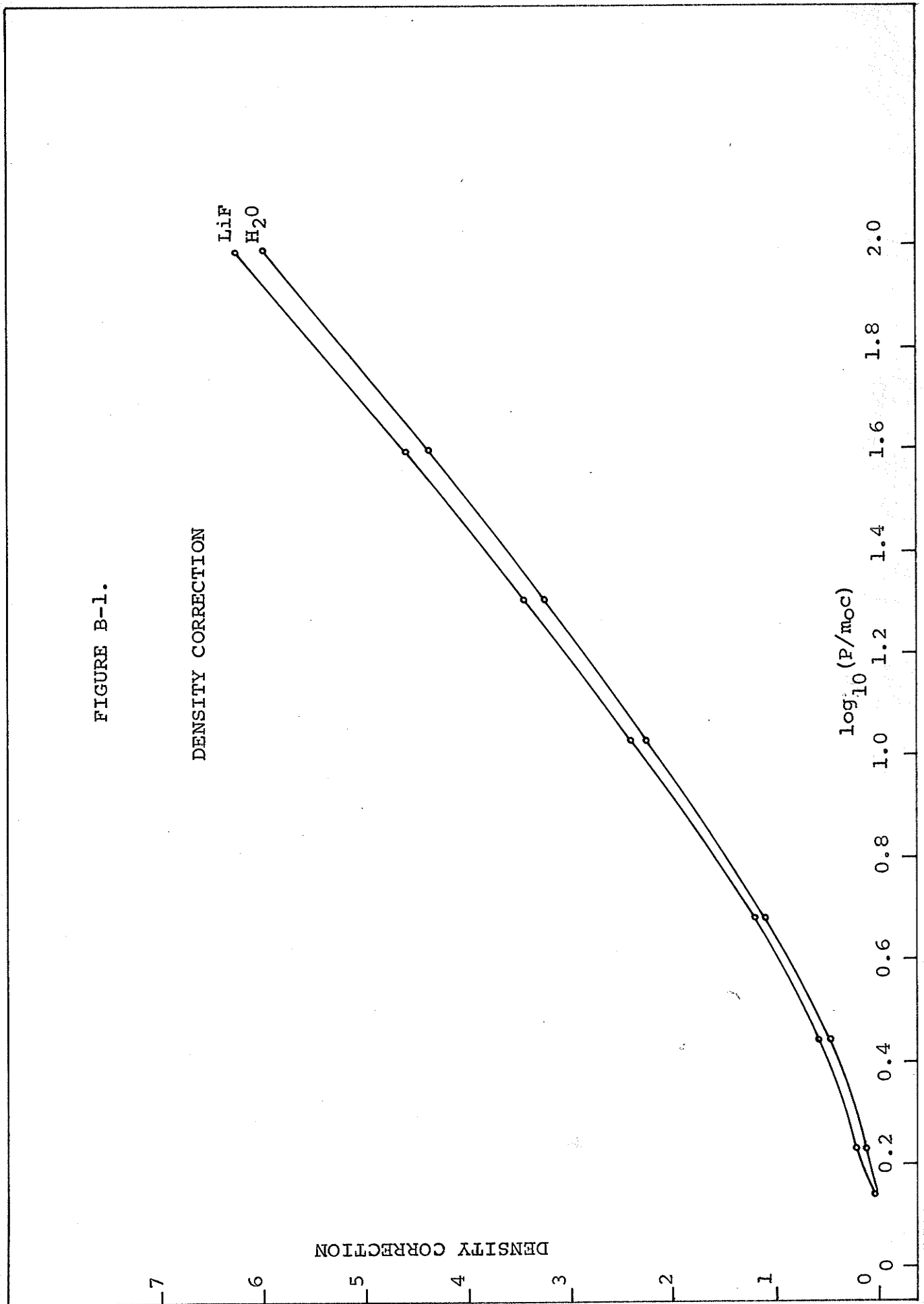
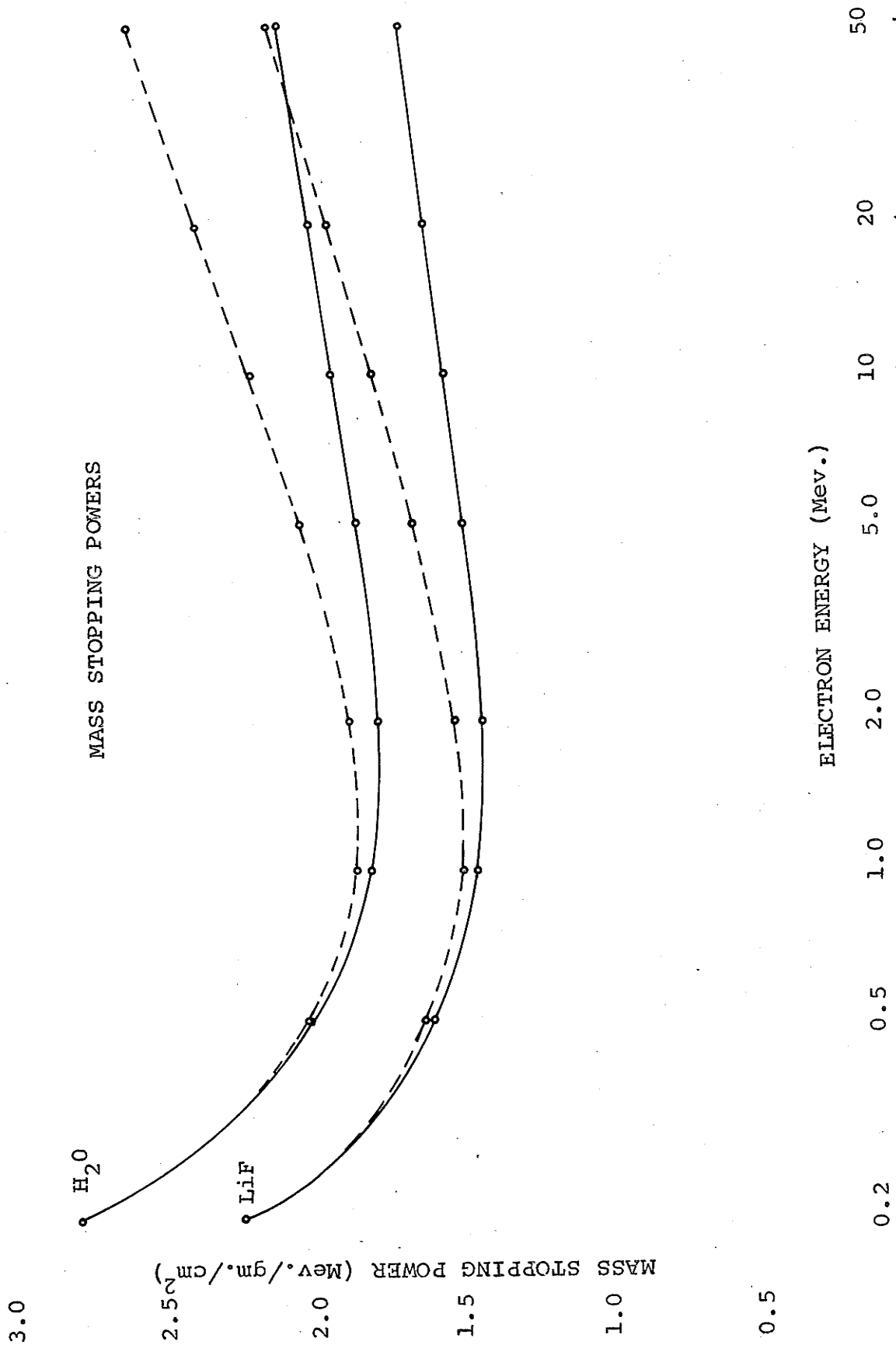


FIGURE B-2.

MASS STOPPING POWERS



ELECTRON ENERGY (MeV.)

MASS STOPPING POWER (MeV·gm./cm.)

H₂O

LiF